THE MORPHOLOGY OF KNM-ER1805:

A Reconsideration of an Enigmatic Specimen

Ricci L. Grossman

Paper submitted in partial fulfillment of the requirement for a non-thesis option Masters Degree

April 2009

_____
Dr. Sheela Athreya, Chair

_____
Dr. Darryl de Ruiter, Member

_____
Dr. James Woolley, Member

ABSTRACT

In the past, KNM-ER 1805 has been designated as a paratype for *Homo erectus, H. ergaster, H. habilis*, and *H. rudolfensis*. Based on its stratigraphic position within the KBS layer (~1.85mya) of the Koobi Fora Formation, this specimen can be temporally associated with all of these taxa, and with *Paranthropus boisei*. Although the majority of researchers attribute KNM-ER 1805 to the genus *Homo*, some suggest it might be more appropriately allocated to *Paranthropus* or *Australopithecus*, thus this issue remains unresolved. This study examines 27 metric and 122 non-metric cranial and mandibular features of several groups of African Plio-Pleistocene hominins to determine the phylogenetic status of KNM-ER 1805 relative to contemporary hominin taxa. It employs multivariate exploration techniques (principal components and discriminant function analyses) and phylogeny reconstruction methods: CONTML for continuous characters as well as PAUP* (parsimony) and MrBayes (Bayesian analysis) for discrete characters. Results of the multivariate analyses reveal an association between KNM-ER 1805 and specimens allocated to *A. africanus, H. habilis,* and *H. ergaster*. Cladograms produced from the phylogenetic analyses show little resolution, but in each instance where a clear separation between *Homo* and the australopithecines (*Paranthropus* and *Australopithecus*) is revealed, KNM-ER 1805 consistently groups with the australopithecines. These results suggest KNM-ER 1805 is not a typical specimen of *H. habilis/rudolfensis* or *H. erectus/ergaster*, despite the fact that it has been cited as a paratype for each of these taxa. Furthermore, these results suggest the affinity of this enigmatic specimen may not lie with the genus *Homo* at all.

INTRODUCTION

Proponents of the biological species concept consider a species to be comprised of a group of actually or potentially interbreeding organisms (Mayr 1942). This definition works reasonably well in studies of living populations; however, there are no set rules as to the amount of morphological variation tolerated within a given species, and many exhibit high levels of differentiation. These differences may be caused by a variety of factors, including environmental change, interactions within and among species, and random factors such as genetic drift. Observation of these forces aids in the delineation of extant species from one another, although this process may be complicated by factors such as hybridization and reticulation.

Studies of extant species must account for a large number of factors, but studies of paleo-species are necessarily more difficult, as the amount and type of variation encompassed within a fossil species must be determined, without the benefit of observing the organisms as they interact with one another. Variation within a single character, sometimes as specific as the dimensions of a premolar, often play an important role in debates concerning the presence of one or multiple species within the fossil record (Leakey et al. 1964; Robinson 1965; Tobias 1966). Thus, it becomes important to consider all of the variation and their possible interpretations. The questions of how much variation is tolerated within a fossil species, of what causes the variation to occur, and of the ways in which distinct taxa differ in their pattern and degree of variation are the roots of unresolved taxonomic debates within the field of paleoanthropology.

One such debate concerns the taxonomic allocation of the specimen KNM-ER 1805, recovered from the Koobi Fora formation in Kenya. The specimen has been cited as a paratype for *Homo erectus, H. ergaster, H. habilis,* and *H. rudolfensis* (see Wood and Richmond 2000, and references therein). KNM-ER 1805 was recovered from the KBS member of the Koobi Fora

formation, which dates to 1.85 million years ago (hereafter, abbreviated "mya") (Feibel et al. 1989; Wood 1991), placing it in close temporal and geographic association with several other taxa, including *Paranthropus boisei*, *H. habilis* (and *H. rudolfensis*), and African *H. erectus* (also referred to as *H. ergaster*) (Feibel et al. 1989). Previous morphological considerations of KNM-ER 1805 have failed to determine which of these taxa, if any, that the specimen is most like.

Historically, there has been a debate concerning the relatedness of specimens belonging to *H. habilis* and *H. rudolfensis*. Some have argued that individuals allocated to these groups are actually members of the same species, *H. habilis* (Lee 2005; Miller 2000); while others suggest that the variation within individuals allocated to these two groups is great enough to warrant a taxonomic split (Grine et al. 1996; Lieberman et al. 1996). A similar debate exists concerning *H. erectus* in Asia and specimens from Africa that have been referred to as both *H. ergaster* and African *H. erectus* (Anton 2002; Baab 2008; Rightmire 1998). The purpose of this paper is not to delve into these debates; but rather to examine the metric and non-metric cranial and mandibular features of KNM-ER 1805, with the intention of resolving the evolutionary relationship of this specimen to contemporaneous fossil taxa. Thus, the use of species designations, including *H. habilis*, *H. rudolfensis*, *H. erectus*, and *H. ergaster* is in following with those of the original authors from whom the data has been obtained.

BACKGROUND

Uncovered *in situ*, the KNM-ER1805 specimen is comprised of three well-preserved cranial fragments that piece together cleanly, as well as an associated mandible. The relatively large cranium with sagittal and nuchal crests, coupled with relatively small teeth presents a stark

contrast to previously recovered East Rudolf specimens (Leakey 1974; Leakey 1976) and subsequent analyses have yet to unequivocally allocate the remains to a single taxonomic group. The majority of morphological reviews have attributed KNM-ER 1805 to the genus *Homo* (Groves and Mazak 1975; Kimbel et al. 1984; Olson 1978; White et al. 1981; Wolpoff 1978), but some have also suggested that the specimen's affinities may lie with the australopithecines (Falk 1986; Leakey 1976; Tobias 1980).

The specimen is characterized by an elongated neurocranium with moderately thick cranial vault bones, and the presence of parasagittal crests appears to align KNM-ER 1805 with specimens such as KNM-ER 406 and KNM-ER 732 (Wood 1978), both of which have been attributed to *Paranthropus boisei* (Wood and Richmond 2000). However, the presence of relatively large canines may align the specimen more closely with individuals of *H. habilis* (Wood 1978). Other studies of the canine and post-canine tooth size have attributed KNM-ER 1805 to *H. erectus* (Wolpoff 1978) and *H. ergaster* (Groves and Mazak 1975).

In comparisons to other Plio-Pleistocene hominins, the occipital anatomy (Bilsborough and Wood 1986) and the basicranium as a whole (Thompson 1993) have reinforced the affinity of the fossil with specimens allocated to *H. erectus* or *H. ergaster*. However, KNM-ER 1805 lacks the coronal expansion and reduced sagittal dimensions of *H. erectus*, possibly suggesting a closer phenetic relationship with *H. habilis* (Bilsborough and Wood 1986). Other studies have also suggested affinity between the fossil specimen and members of the genus *Homo,* including White et al. (1981) and Kimbel et al. (1984), who provisionally allocated KNM-ER 1805 to *H. habilis* based upon its divergence from the facial and cranial base morphology characteristic of the australopithecines. Thompson (1993) also suggested similarities in the basicranial morphology between KNM-ER 1805 and KNM-ER 3733, KNM-ER 3883, and OH 9 (generally

considered to be members of the *H. erectus/H. ergaster* group), but also KNM-ER 1470 (a member of the *H. habilis/H. rudolfensis* groups).

Dean and Wood (1982) have suggested a close alignment between the cranial base morphology of KNM-ER 1805 and the robust australopithecine *Paranthropus boisei* and Tobias (1980, 1985) allocated the specimen to *P. boisei* on the basis of molar morphology; although previous studies of the molars have suggested similarities with the genus *Homo* (Groves and Mazak 1975). And, studies have not only found similarities between KNM-ER 1805 and the robust australopithecines, but Falk (1983, 1986) suggests that the cerebral cortex morphology and cranial blood drainage pattern may be more like that of the gracile australopithecines (Falk 1983; Falk 1986).

Overall, there is little agreement regarding the taxonomic allocation of KNM-ER 1805, and some researchers have preferred to ultimately relegate this specimen to indeterminate status (Bilsborough and Wood 1986; Kimbel and Rak 1985; Wood and Abbott 1983; Wood et al. 1988; Wood and Engleman 1988). However, understanding the taxonomy and morphology of KNM-ER1805 is important because of its location at Koobi Fora and its association with remains attributed to *P. boisei, H. habilis, H. rudolfensis,* and *H. ergaster* (Feibel et al. 1989). Allocation of KNM-ER1805 to any of these species influences our understanding of the range of morphological variation within these populations, as the cranium possesses some characteristics that are wholly different from what is considered "typical" for *Paranthropus* or early *Homo.*

Previous studies of ER1805 have focused on the size and shape of the mandible and post-canine dentition (Chamberlain and Wood 1985; Groves and Mazak 1975; Leakey 1976; Tobias 1980; White et al. 1981; Wood and Abbott 1983; Wood et al. 1988), features of the frontal and occipital bones (Kimbel et al. 1984; White et al. 1981), and endocranial features (Falk 1983; Falk

1986). These analyses have been limited by their focus on only a few characteristics from a specific region of the skull. Studies have shown that focusing analyses on a single character, character complex, or morphological region is likely to reveal different phylogenetic relationships depending upon the trait or complex used (Tobias 1985). Therefore, the purpose of this study is to consider the cranial and mandibular morphology of KNM-ER1805 in its entirety, as represented by linear metrics and numerically coded cladistic characters, with respect to other African hominins, in order to gain a better understanding of its phylogenetic relationship to other fossil hominins.

MATERIALS AND METHODS

Sample

Linear cranial measurements obtained from a sample of Plio-Pleistocene African hominin taxa, including KNM-ER 1805, along with several extant African hominoids are utilized in several multivariate analyses. Fossil specimens included in the data set are limited to adult individuals of comparative interest to KNM-ER 1805, specifically those species to which it has been compared or allocated, along with those that are roughly geographically or chronologically contemporaneous (Table 1). These include *A. africanus, P. boisei, P. aethiopicus, H. habilis, H. rudolfensis, H. erectus,* and *H. ergaster*. The extant ape sample consists of individuals from *Pan* and *Gorilla*.

Specific taxonomic allocation for each specimen included in the analysis has been determined *a priori* based upon reference to current literature (see Table 1). For purposes of this study, *H. habilis* and *H. rudolfensis* have been treated as separate species, as have *H. ergaster*

and *H. erectus.* The treatment of these two groups as each representing one or multiple species is highly debated (Kramer 1993; Lieberman et al. 1996; Miller 2000; Rightmire 1998); thus the designations use in this study are based upon those of (Prat 2002, 2005), from whom a portion of the data for this analysis is taken.

In addition to multivariate analysis, a numerical cladistic analysis is also performed using an early hominin data set extracted from Prat (2005). The Plio-Pleistocene specimens included in this analysis are also limited to individuals of comparative interest to KNM-ER 1805. Species included in the analysis are *H. habilis, H. rudolfensis, H. erectus, H. ergaster, P. boisei, P. robustus, A. africanus,* and *A. afarensis*, as well as members of *Pan* and *Gorilla* (Table 2). Although many individuals included in the set are generally agreed to be members of particular fossil species, there is a lack of consensus for all individuals. Therefore, each specimen in the cladistic analysis has been considered independently as its own taxonomic unit. The data set contains numerical cladistic coding for 122 cranial and mandibular features from 23 fossil specimens plus two extant ape taxa (Table 3).

The multivariate data consists of 20 cranial measurements from 39 fossil specimens and 7 mandibular measurements form 35 fossil specimens (Wolpoff, personal communication; see Table 4 for a list of measurements). All measurements are from the original fossil specimens, except for the single mandibular specimen AL-333W-1, whose measurements are from a cast of the original fossil and were taken by Wolpoff. Measurements of extant apes were taken by the author. In order to maximize the sample of fossil hominins for comparison, the mandibular and cranial measurement data sets are treated separately, and there are some differences in the specimens retained for comparison in each group.

It should also be noted that the samples used in the morphometric analysis and the cladistic analysis are not identical. The cladistic data set includes two specimens (OH 62 and STW 505), for which the linear measurements used in this study were not available. Additionally, there are more individuals included in the multivariate data set than in the individually coded cladistic data, which results from a lack of published data, as many cladistic studies do not consider the individual as the operational taxonomic unit. Therefore, the results of analyses presented here should be considered preliminary, as they are based only on these available data. Future research should incorporate use of equivalent data sets, allowing more accurate comparison of the results obtained in the morphometric and cladistic analyses.

Multivariate Analyses

For the cranial and mandibular data obtained from the fossil specimens, missing data values were imputed using NORM version 2.03 (Schafer 1999). NORM is a multiple imputation program that uses a two-step process to impute missing data values, beginning with expectation maximization (EM). The EM algorithm is based upon maximum likelihood estimation (MLE) and is generally considered to be superior to other multivariate regression techniques for imputing missing data values in craniometric analyses (Kramer and Konigsberg 1999). Due to missing values in the data set, a small amount of prior information must be introduced in order for convergence under the EM algorithm to occur; this is achieved using a ridge prior (hyperparameter = 2) to shrink estimated correlations (Schafer 1997). The second phase of imputation, data augmentation (DA), is an iterative process that uses a random imputation to draw new parameters from a Bayesian posterior distribution, creating a Markov Chain that eventually converges (Schafer and Olsen 1998). After convergence of the DA phase, multiple

imputation yielded a total of four sets of values for the missing data in both sets, and these values were averaged to create the complete data sets used here.

To more effectively evaluate shape similarities, the data was transformed using the geometric mean (Darroch and Mosimann 1985) to create scale-free geometric components that minimize the effects of size. A principal components analysis was performed using SPSS version 15.0 on the raw and transformed data sets. Each component accounting for 1% or more of the total variance within the data was retained and utilized in subsequent analyses. As craniometric variables are generally highly correlated with one another, these new orthogonal variables are useful in analyses that require data to be uncorrelated, such as discriminant function analyses.

Discriminant function analysis (DFA) was performed on each of the principal component data sets. DFA presupposes that we can divide out observations into groups on the basis of some criterion and then finds ways to distinguish those same groups based on some other independent criterion derived from the data (Shennan 1997). For this analysis, the group assignment for KNM-ER 1805 was left blank to allow the DFA to determine the most likely assignment for the individual, and posterior and typicality probabilities were obtained for each group assignment given to KNM-ER 1805.

The orthogonal principal component variables were also used in constructing a maximum likelihood tree using the CONTML module of Phylip version 3.68 (Felsenstein 2004b). The relationship tree produced from these uncorrelated variables should yield the most accurate relationship tree (given the data at hand) based on the morphological similarity between the specimens examined. Since the order of data input can affect the outcome of the maximum likelihood analysis in CONTML, the data sets were analyzed 25 times and the input order of the

variables randomized for each analysis. Global rearrangements were also performed in each analysis to ensure that the trees with the highest likelihood were recovered.

Cladistic Analyses

The cladistic analyses performed here involve both a maximum parsimony and Bayesian inference approach. Parsimony seeks to find the cladogram requiring the fewest possible state changes to explain the data, and this approach typically performs well as long as the taxa of interest possess a relatively small number of convergent traits (Holder and Lewis 2003). Maximum parsimony is a common approach to the analysis of morphological data from fossil taxa (Lieberman et al. 1996; Prat 2002; Prat 2005; Smith and Grine 2008; Strait and Grine 2004; Strait et al. 1997), and the analysis performed here is an attempt to recreate results originally obtained by Prat (2002, 2005).

Parsimony analysis was performed using the program PAUP* (version 4.10b; Swofford 2003) using the data obtained from Prat (2005). Following Prat (2005), missing data was treated as "missing," character states were considered un-ordered and non-additive, and multiple character states were coded as "polymorphism" instead of "character state uncertainty." Branches with a minimum length of zero were collapsed in order to reduce the number of redundant trees and the addition sequence was set to random with a randomly selected starting seed. The number of random addition sequences originally performed by Prat (2002, 2005) was not specified; so a preliminary search with 10,100, and 1000 random addition sequences was performed to determine the most appropriate number. The results of this search indicated that the number of equally parsimonious trees increased as the number of addition sequences increased,

thus the number of random addition sequences was set to 1000 for all analyses to ensure that all possible trees were examined.

As a measure of branch support, the Bremer decay index was computed for each node of interest in the consensus trees produced by the parsimony analysis (Bremer 1994). Additionally, the ensemble consistency index (CI) was calculated for each tree; the CI measures the frequency of parallelism (homoplasy as a fraction of the total character change) (Farris 1989).

Bayesian inference analysis was performed using the program MrBayes 3.1.2 (Ronquist and Huelsenbeck 2003). Although closely related to maximum likelihood analysis, a common approach to analyzing morphological data within the anthropological literature (Athreya and Glantz 2003; Gonzalez-Jose et al. 2008; Kramer and Konigsberg 1999), Bayesian methods are relatively novel at this time. Typically, Bayesian inference methods are applied in molecular analyses using DNA sequences to determine phylogeny. However, Lewis (2001) has suggested that Bayesian methods are equally applicable to discrete morphological data sets because the maximum likelihood function is the foundation of the analysis. Bayesian inference offers a means for obtaining meaningful measures of nodal support while minimizing the computational burden involved in considering all possible phylogenetic trees by sampling the trees according to their posterior probabilities (Huelsenbeck et al. 2000; Larget and Simon 1999; Lewis 2001).

Bayesian methods rely primarily upon a Markov Chain Monte Carlo (MCMC) algorithm, which approximates probability distributions by taking a random sample from the posterior distribution of all possible trees given the data (Felsenstein 2004a). The MCMC works by taking a series of steps through parameter space forming a conceptual chain. At each step along the way, the proposed “next link” is generated by a random perturbation of the current parameters (Holder and Lewis 2003), and if the tree created by the parameter settings at this new location

has a higher posterior probability than the previous position, that tree is accepted and becomes the new present state of the chain, and this process is repeated for millions of generations via the Metropolis-Hastings algorithm (Felsenstein 2004a). By design, the Markov chain will stay in regions of parameter space where the posterior probabilities are high, and the proportion of time spent in these regions is used as an estimate of the posterior probability of those regions (Holder and Lewis 2003). This posterior probability is generally representative of an intuitive measure of confidence in the given tree for those parameters.

In this analysis, two Bayesian analyses with four chains each were run for two million steps after starting from a random tree, with samples taken every 1000 generations. The Markov chains were determined to have converged when the standard deviation of split frequencies (SDSF) of the two independent chains fell below 0.01 (Tinn and Oakley 2008). The steps taken prior to convergence are removed from the analysis as the "burn-in."

RESULTS

Multivariate Analysis

Principal Components Analysis

A principal components analysis (PCA) using SPSS is achieved by running the factor analysis (FA) module with a principal component extraction setting, for which the communalities are set to 1.0 before proceeding with a factor analysis. Under these conditions, the FA is equivalent to having run PCA on the correlation matrix of the data (Johnson 1998). Principal component analysis of the untransformed cranial data set extracted four components with eigenvalues greater than 1.0, explaining a total of 81.48% of the total data variance, and ten

components that describe greater than 1% of the total variance, accounting for a total of 96.24% of the variance within the data (Table 5). PC analysis of the untransformed mandibular data extracted two components with eigenvalues greater than 1.0 and five components that account for more than 1% of the data variance, accounting for 85.83% and 98.76% of the total variance, respectively (Table 6). Analysis of the transformed cranial data set extracted six components with eigenvalues greater than 1.0, explaining a total of 79.28% of the total data variance. A total of twelve components describe greater than 1% of the total variance in the data, which explains a total of 96.19% of the variation (Table 7). Finally, the transformed mandibular data set yielded three components with eigenvalues greater than 1.0 and six components explaining greater than 1% of the total variance, accounting for 87.09% and 100% of the variance within the data set (Table 8).

Discriminant Function Analysis

Discriminant function analyses (DFA) were performed on the retained principal components for each of the four data sets (raw cranial, raw mandible, transformed cranial, and transformed mandible). The analysis of the raw cranial data set yielded three functions with eigenvalues greater than 1.0 (94.6% of the variance), each of which is significant at the p=0.000 level. A scatterplot of the first two functions shows a clear separation of *Pan* and *Gorilla* from the remaining individuals (Figure 1a); however, the apes are plotting so far from the remaining hominins that it is difficult to distinguish any groupings present in the other fossil individuals. By focusing more specifically on the region of the scatterplot occupied by the hominins (Figure 1b), more discrete groupings can be seen.

Analysis of the untransformed mandibular data set yielded two functions with eigenvalues greater than 1.0 (90.5% of the variance), both of which are significant at the level of p=0.000. The scatterplot of discriminant functions one and two show a very clear separation of *Gorilla*, but less so with *Pan* (Figure 2a). A focused examination of the scatterplot (Figure 2b) reveals more clarity in the groupings of the fossil hominins examined in this study, but also shows that KNM-ER 1805 is not similar to the others in its untransformed mandibular measurements.

The transformed cranial data yielded four functions with eigenvalues greater than 1.0 (97.3% of the total variance, and all four of the functions are significant (the first three at p=0.000, the fourth at p=0.005). A scatterplot of the first two functions reinforces the separation of *Pan* and *Gorilla* from the fossil individuals (Figure 3a); but a more focused scatterplot reveals the separation among the comparative hominin sample (Figure 3b). Finally, the transformed mandibular data yielded two functions with eigenvalues greater than 1.0 (87.7% of the total variance), and both are significant (the first at p=0.000, the second at p=0.001). The scatterplot of these two functions also shows a clear separation between *Pan* and *Gorilla* and the remaining individuals (Figure 4a); and the scatterplot that focuses more on the fossils (Figure 4b) highlights the separation among them, and reinforces how different KNM-ER 1805 is in its mandibular morphology. The group memberships suggested by all four of these analyses include *A. africanus, H. erectus* and *H. habilis.* These findings, along with their posterior and typicality probabilities are summarized in table 9.

CONTML Analysis

The maximum likelihood analysis performed using CONTML on the orthogonal components retained from the initial PCA yielded trees with vastly different groupings of specimens. In all cases, *Pan* separated from the remaining individuals first and *Gorilla* much later. A visual inspection of the trees reveals a notable absence of individuals allocated to the same species groups clustering together. Additionally, it appears that KNM-ER 1805 occupies a different position in every tree.

For the raw cranial data, KNM-ER 1805 separates from the remainder of the specimens very early and is grouped with individuals allocated to *A. africanus* (MLD 37) and *H. rudolfensis* (KNM-ER 3732) (Figure 5). In the tree created from the transformed cranial data, KNM-ER 1805 separates relatively late and is grouping with two of the Dmanisi specimens (Dmanisi 2700 & 2280), both of which have been allocated to *H. erectus* (Figure 6).

Analysis of the raw mandibular data yields a tree in which KNM-ER 1805 is grouped in a node with individuals allocated to *H. habilis* (OH 37), *H. rudolfensis* (KNM-ER 1801 and KNM-ER 1482), *H. ergaster* (KNM-ER 992), *H. erectus* (Dmanisi 2282, BK 67, and Ternifine 1 and 2), along with the three *Gorilla* specimens (Figure 7). At this node, KNM-ER 1805 is separated from these other specimens, and seems to be most closely associated with OH 37 (*H. habilis*). Finally, the transformed mandibular data yields a tree in which KNM-ER 1805 is grouping with individuals allocated to *H. habilis* (OH 37), *H. rudolfensis* (KNM-ER 1483), and *H. ergaster* (OH 51) (Figure 8).

Cladistic Analysis

Parsimony

The cladistic analysis presented here was initially undertaken to explore the results found in previous studies by Prat (2002, 2005), which yielded three most parsimonious trees with a length of 431 steps (Figure 9). Using the same data and following Prat (2005), a parsimony search in PAUP* (version 4.10b) was performed to recreate these results. *Pan* and *Gorilla* were set as an outgroup to the remainder of the fossil specimens and the parsimony option for collapsing minimum branch lengths to zero was selected to reduce redundancy. The addition sequence for the heuristic search was random addition with a randomly selected starting seed. This parsimony search, performed with 1000 replications of the random addition sequence, yielded a single most parsimonious tree with a length of 429 steps (Figure 10).

Bayesian Inference

The Bayesian analysis was performed usingthe MrBayes 3.1.2 program, with a symmetric dirichlet fixed variance parameter, all topologies equally probable, and unconstrained branch lengths (default settings for morphological data). The analysis is two simultaneous, independent runs starting from two different random trees, and the Markov Chain Monte Carlo (MCMC) analysis ran for two million replications. In the analysis, the average standard deviation of split frequencies (SDSF) was 0.006456 by the two millionth step, with no burn-in established, and the Potential Scale Reduction Factor (PSRF) was equal to 1.001, suggesting that the runs were reaching convergence (PSRF should approach 1 as the runs converge) (Gathogo and Brown 2006). The burn-in was set to the point where the SDSF falls permanently below 0.01 (Tinn and Oakley 2008), at 589,000 steps (burn-in = 589) and after accounting for the burn-in, the PSRF is

still 1.001. The consensus tree with the clade credibility values (Figure 11) gives the probability of each clade in the tree.

DISCUSSION

Previous morphometric examinations of KNM-ER1805 have failed to unequivocally allocate the specimen to any African hominin species. Morphological examinations of KNM-ER 1805 have attributed it to *H. ergaster, H. erectus, H. habilis, P. boisei,* and *Australopithecus africanus*. Unfortunately, the results of metric analyses presented here, coupled with maximum parsimony and Bayesian inference, do not clearly support any single taxonomic allocation for KNM-ER1805.

The DFA suggests that the highest posterior probability of membership for the fossil specimen is with either *A. africanus, H. ergaster,* or *H. habilis,* depending on whether one considers the raw or transformed variables (Table 9). However the typicality probability for allocation of this specimen to any of these groups is very low, only 2.6% for the raw cranial data, 11.6% for the transformed cranial data, and 0% for either of mandibular data sets. These low typicality probabilities suggest that KNM-ER 1805 is not typical of any of the groups to which it has been assigned.

The CONTML analysis reveals a similar result, yielding four different trees depending on the data set used; none of which show a clear separation between the australopithecines and the genus *Homo.* The association of KNM-ER 1805 changes in each tree, but is roughly coincident with the results of the DFA – also suggesting similarity with specimens allocated to *A. africanus, H. habilis,* and *H. erectus.*

Results from the cladistic analyses are not any clearer. The maximum parsimony approach yielded a single most parsimonious tree of 429 steps, which differs from the results obtained by Prat (2002, 2005). The results of the parsimony analysis performed by Prat (2002, 2005) (Figure 9) indicate the presence of two distinct clades separated at node A, the australopithecines and *Homo*, with KNM-ER 1805 grouping near several specimens attributed to *P. boisei* and *P. robustus*. As interpreted by Prat (2002), these results suggest that KNM-ER 1805 falls into a peculiar position, linked at node D with two specimens allocated to *P. boisei* (KNM-ER 406 and OH 5) and two specimens attributed to *P. robustus* (SK 48 and SK 46), but not with any specimen of the *Homo* clade (defined at node A). Overall, her results suggest that KNM-ER 1805 does not belong to the *Homo* clade, making it an inappropriate morph for early *Homo* in cladistic analyses or morphological comparisons.

Although KNM-ER 1805 also groups with members of *Paranthropus*, the result obtained in the analysis performed here (Figure 10) differs from that obtained by Prat (2002, 2005). Besides the length difference between the two trees, several individuals that group with the australopithecine clade in Prat's analysis are separated as a sister taxa to the remaining individuals in this analysis: AL 333-45 (*A. afarensis*) and KNM-WT 17000 (*P. boisei/P. aethiopicus*). Additionally, a single australopithecine, Stw 505 (*A. africanus*) appears to be grouping with many individuals attributed to *Homo* at node A, while the remainder of the australopithecines are grouped together at node B.

The inability of this study to replicate results obtained by Prat (2002, 2005) may be the result of several factors. First, the number of addition sequences used in the parsimony analysis by Prat (2002, 2005) was not specified. A preliminary search with 10, 100, and 1000 random addition sequences suggested that the number of equally parsimonious trees increased as the

number of addition sequences increased. Because of this, the number of random addition sequences was set to 1000 to maximize the number of trees examined and the number used by Prat (2002,2005) may have been different. Second, the search algorithm used by Paup* (version 4.10b, used in this analysis) is slightly changed from the algorithm used in Paup 3.1 (utilized by Prat 2002,2005) (Swofford 2003). The analysis performed here should be more robust due to the improved search algorithm in the current implementation of Paup*, but the different algorithm could also be contributing to the differences between the analyses.

The Bremer's decay index was calculated to evaluate nodal support for this tree and it does not suggest a particularly strong relationship between the clades presented here. Bremer support values represent the difference in length between the tree presented and the next shortest tree without the clade of interest; so a support index of 1.0 suggests that there is at least one tree only one step longer in which the clade of interest is not present. Additionally, the CI for the tree obtained in this analysis (0.4522) is the same as that of Prat's analysis (0.452), suggesting that the amount of homoplasy and homology detected in the trees is similar between the two analyses.

On the whole, the Bayesian analyses produced a consensus tree with relatively high posterior probability for a nearly completely unresolved tree (Figure 11). The Bayesian tree suggests a 100% posterior probability that the fossil taxa are distinct from the extant primate outgroups, a result that is not at all unexpected. What is unexpected, however, is the absolute lack of resolution in the remainder of the tree. The four clade relationships proposed in the tree – associations between OH 24 and OH 13, between KNM-ER 3733 and KNM-ER 3883, between STS 5 and STS 71, and between SK 46 and SK 48 – are well supported, with the lowest posterior

probability being 0.53 (or 53%); however, these relationships are not particularly enlightening, as each individual in these pairs is associated with the same taxon as the other.

If these trees are an accurate reflection of the phylogenetic relatedness of the individuals, then parsimony analysis suggests the affinity of KNM-ER 1805 may lie with the australopithecines. However, the reliability of the phylogenies produced here must be questioned, as the parsimony tree presented must be questioned, as the parsimony tree produced here is not well supported by Bremer's decay index and the Bayesian analysis reveals high measures of nodal support (posterior probabilities), but the tree has little resolution, which may indicate a lack of phylogenetic signal within the cladistic data. Additionally, these results differ from those suggested by the multivariate methods which show similarity between KNM-ER 1805 and either *Homo* or the gracile australopithecine *A. africanus*.

To better understand the morphological characters contributing to the position of KNM-ER 1805, trait histories were traced using the Mesquite program (Maddison and Maddison 2007) to examine the maximum parsimony tree (Figure 10). Examination of the character state changes leading to the proposed tree suggest that several features are preventing KNM-ER 1805 from grouping within the *Homo* clade, including strong postorbital constriction, the moderate level of lateral development of the supramastoid crest, the junction between the mastoid and supramastoid crests (present), and the position of the posterior root of the zygomatic process. Additionally, the strong development of the juxtamastoid eminence, a superior-anterior to inferior-posterior orientation of an elliptical external auditory meatus, the anterior position of the foramen magnum (relative to the bitympanic line), and a compounding of the temporal/nuchal crests are also pulling KNM-ER 1805 over to the australopithecine group (at node C).

Despite grouping with the australopithecines in this analysis, reconstruction of the character state history for the individual suggests that KNM-ER 1805 shares some traits with members of the genus *Homo*, including presence of a prelambdoid depression, which is shared with KNM-ER 3733 and KNM-ER 3883 only. Additionally, KNM-ER 1805 possesses strong "mastoid crest individualism" (Prat 2005), which is shared with KNM-ER 1470, KNM-ER 3732, KNM-ER 730, OH 9, and WT 17000. KNM-ER 1805 also possesses several unique traits that distinguish it from all or nearly all other specimens considered in the analysis. The diamond shape of the temporomandibular joint is shared only with KNM-ER 1470 and the rectangular shape of the postglenoid process is shared only with KNM-ER 1813. Two unique traits for KNM-ER 1805 identified by Mesquite include projection of the nasal bones at the same level as the frontomaxillary suture (all other specimens project above the level of the suture, except for WT 17000 which is below) and the presence of a metopic crest.

Interestingly, not all descriptions of KNM-ER 1805 describe the individual as possessing a metopic crest, as authors such as Thompson (1993) and White et al. (1981) have described the persistence the metopic suture with no reference to cresting in the individual. A persistent metopic suture is considered normal variation within Plio-Pleistocene hominins and has been described Sts 5, KNM-ER 1813, KNM-ER 3733, KNM-ER 3883, WT 15000, and OH 24 (Prat 2002). Re-running the parsimony analysis with KNM-ER 1805 character states altered to reflect an absence of the metopic crest and reduction of the sagittal crest, still does not group the individual with individuals attributed to the genus *Homo,* so these characters must not be responsible for defining the affinity between KNM-ER 1805 and the australopithecines.

Historically, there has been great issue with defining characteristics that must be present in members of the genus *Homo*. Wood (1992) has suggested that there are eight defining

characteristics that should be present in members of the genus. These include: increased cranial vault thickness, reduced post-orbital constriction, an increased contribution of the occipital bone to overall sagittal arc length, increased cranial vault height, a more anterior position of the foramen magnum, reduced lower face prognathism, narrower tooth crowns (particularly in the premolars), and a reduced overall length of the molar tooth row (Wood 1992). Of these eight characteristics, only three have been considered in the cladistic analyses presented here: degree of postorbital constriction, foramen magnum position, and degree of facial prognathism.

With respect to these characters, there is a problem with the character state coding for KNM-ER 1805 with respect to facial prognathism (this is coded as "?" in the cladistic data set). Additionally, Wood (1992) suggests that the genus *Homo* is defined by a more anterior location of the foramen magnum; however, the cladistic coding for this character suggests that KNM-ER 1805 possesses an anteriorly located foramen magnum (relative to the bitympanic line), a characteristic that is shared with other australopithecines, while the members of the genus *Homo* are characterized by a posteriorly position foramen magnum (except WT 17000 and KNM-ER 3883, whose foramen magnum position is even with that of the bitympanic line). So, there must be some difference in the definition of an "anteriorly placed foramen magnum" between Wood (1992) and Prat (2002, 2005). The final characteristic of the genus *Homo*, decreased postorbital constriction is not a characteristic of KNM-ER 1805.

Therefore, it seems that the cladistic data set considered here may be lacking some of the relevant character states required to fully understand the phylogenetic position of KNM-ER 1805 with respect to other Plio-Pleistocene hominins. If one considers that the multivariate analyses may arguably suggest more of an affinity between KNM-ER 1805 and members of the genus *Homo*, then it becomes even more relevant that we understand the morphology of this

unallocated specimen with respect to the defining characteristics of the genus *Homo* (as discussed by Wood 1992), and this should be an avenue of research explored in the future.

CONCLUSIONS

Previous morphological analyses of KNM-ER 1805 have failed to consistently associate the specimen with any contemporaneous Pleistocene hominin group, including those to which it has been previously allocated, suggesting that this fossil exhibits a combination of morphological characters unlike that known for any other fossil specimen. Results presented here suggest KNM-ER 1805 is not a typical specimen of *H. habilis/H. rudolfensis* or *H. erectus/H. ergaster,* despite that it has been cited as a paratype for each of these taxa (see Wood and Richmond 2000, and references therein), nor is its morphology typical of *Paranthropus* (Prat 2002).

If we consider that the morphological and/or genetic changes characteristic of evolution must first occur in the *individual* before characterizing a population or species, then the individual must be the starting point for any significant evolutionary shift. It is within this context, that KNM-ER 1805 becomes most interesting. Factors such as the co-existence of several bipedal hominin taxa in East Africa and the expansion of *H. erectus/ergaster* outside of Africa nearly 1.8mya must have played a role in shifting the inter- and intra-specific interactions occurring in these hominin groups.

Although it is likely that the evolutionary processes working in East Africa, nearly two million years ago, are more complex than we currently understand, the suite of traits present in KNM-ER 1805 are certainly unique, and may be a reflection of these evolutionary shifts. Detailed morphological study of KNM-ER 1805, and other specimens like it, have great

potential for increasing our knowledge and understanding of morphological variation within the Pleistocene, as well as for helping to elucidate the complexities of the evolutionary process. Ultimately, it is important to understand that the results of any analysis using KNM-ER 1805 will be affected by the group within which we place this specimen.

REFERENCES

Alemseged Z, Coppens Y, and Geraads D. 2002. Hominid cranium from Omo: Description and taxonomy of Omo-323-1976-896. American Journal of Physical Anthropology 117(2):103-112.

Anton SC. 2002. Evolutionary significance of cranial variation in Asian Homo erectus. American Journal of Physical Anthropology 118(4):301-323.

Anton SC. 2003. Natural History of *Homo erectus*. Yearbook of Physical Anthropology 46:126-170.

Athreya S, and Glantz MM. 2003. Impact of character correlation and variable groupings on modern human population tree resolution. American Journal of Physical Anthropology 122(2):134-146.

Baab KL. 2008. The Taxonomic Implications of Cranial Shape Variation in *Homo erectus*. Journal of Human Evolution 54(827-847).

Bilsborough A, and Wood B. 1986. The Nature, Origin and Fate of *Homo erectus*. In: Wood B, Martin L, and Andrews P, editors. Major Topics in Primate and Human Evolution. New York: Cambridge University Press. p 295-316.

Bremer K. 1994. Branch Support and Tree Stability. Cladistics 10:295-304.

Chamberlain AT, and Wood BA. 1985. A Reappraisal of Variation in Hominid Mandibular Corpus Dimensions. American Journal of Physical Anthropology 66(4):399-405.

Darroch JN, and Mosimann JE. 1985. Canonical and Principal Components of Shape. Biometrika 72(2):241-252.

de Ruiter DJ, Steininger CM, and Berger LR. 2006. A cranial base of Australopithecus robustus from the Hanging Remnant of Swartkrans, South Africa. American Journal of Physical Anthropology 130(4):435-444.

Dean MC. 1985. The Eruption Pattern of the Permanent Incisors and 1st Permanent Molars in Australopithecus (Paranthropus) Robustus. American Journal of Physical Anthropology 67(3):251-257.

Falk D. 1983. Cerebral Cortices of East-African Early Hominids. Science 221(4615):1072-1074.

Falk D. 1986. Evolution of Cranial Blood Drainage in Hominids - Enlarged Occipital Marginal Sinuses and Emissary Foramina. American Journal of Physical Anthropology 70(3):311-324.

Farris JS. 1989. The Retention Index and the Rescaled Consistency Index. Cladistics-the International Journal of the Willi Hennig Society 5(4):417-419.

Feibel CS, Brown FH, and Mcdougall I. 1989. Stratigraphic Context of Fossil Hominids from the Omo Group Deposits - Northern Turkana Basin, Kenya and Ethiopia. American Journal of Physical Anthropology 78(4):595-622.

Felsenstein J. 2004a. Inferring Phylogenies. Sunderland, MA: Sinauer Associates, Inc.

Felsenstein J. 2004b. PHYLIP (Phylogeny Inference Package) version 3.68. Distributed by the author Department of Genome Sciences, University of Washington, Seattle.

Gabunia L, Vekua A, Lordkipanidze D, Swisher CC, Ferring R, Justus A, Nioradze M, Tvalchrelidze M, Anton SC, Bosinski G and others. 2000. Earliest Pleistocene hominid cranial remains from Dmanisi, Republic of Georgia: Taxonomy, geological setting, and age. Science 288(5468):1019-1025.

Gathogo PN, and Brown FH. 2006. Revised stratigraphy of Area 123, Koobi Fora, Kenya, and new age estimates of its fossil mammals, including hominins. Journal of Human Evolution 51(5):471-479.

Gonzalez-Jose R, Escapa I, Neves WA, Cuneo R, and Pucciarelli HM. 2008. Cladistic analysis of continuous modularized traits provides phylogenetic signals in Homo evolution. Nature 453(7196):775-U774.

Grine FE, Jungers WL, and Schultz J. 1996. Phenetic affinities among early Homo crania from East and South Africa. Journal of Human Evolution 30(3):189-225.

Groves CP, and Mazak V. 1975. An Approach to the Taxonomy of the Hominidae: Gracile Villafranchian Hominids of Africa. Casopis Pro Mineralogii A Geologii 20:225-247.

Holder M, and Lewis PO. 2003. Phylogeny estimation: Traditional and Bayesian approaches. Nature Reviews Genetics 4(4):275-284.

Holloway RL. 1981. The Endocast of the Omo L338y-6 Juvenile Hominid - Gracile or Robust Australopithecus. American Journal of Physical Anthropology 54(1):109-118.

Huelsenbeck JP, Rannala B, and Masly JP. 2000. Accommodating phylogenetic uncertainty in evolutionary studies. Science 288(5475):2349-2350.

Huffman OF. 2001. Geologic context and age of the Perning/Mojokerto Homo erectus, East Java. Journal of Human Evolution 40(4):353-362.

Johnson DE. 1998. Applied Multivariate Methods for Data Analysts. Pacific Grove, CA: Brooks/Cole Publishing Company. 567 p.

Kimbel WH, and Rak Y. 1985. Functional-Morphology of the Asterionic Region in Extant Hominoids and Fossil Hominids. American Journal of Physical Anthropology 66(1):31-54.

Kimbel WH, White TD, and Johanson DC. 1984. Cranial Morphology of Australopithecus-Afarensis - a Comparative-Study Based on a Composite Reconstruction of the Adult Skull. American Journal of Physical Anthropology 64(4):337-388.

Kramer A. 1993. Human Taxonomic Diversity in the Pleistocene - Does Homo-Erectus Represent Multiple Hominid Species. American Journal of Physical Anthropology 91(2):161-171.

Kramer A, and Konigsberg LW. 1999. Recognizing species diversity among large-bodied hominoids: a simulation test using missing data finite mixture analysis. Journal of Human Evolution 36(4):409-421.

Larget B, and Simon DL. 1999. Markov chain Monte Carlo algorithms for the Bayesian analysis of phylogenetic trees. Molecular Biology and Evolution 16(6):750-759.

Leakey LSB, Napier JR, and Tobias PV. 1964. New Species of Genus Homo from Olduvai Gorge. Nature 202(492S):7-9.

Leakey MG, Spoor F, Brown FH, Gathogo PN, Kiarie C, Leakey LN, and McDougall I. 2001. New hominin genus from eastern Africa shows diverse middle Pliocene lineages. Nature 410(6827):433-440.

Leakey REF. 1974. Further Evidence of Lower Pleistocene Hominids from East Rudolf, North Kenya, 1973. Nature 248(5450):653-656.

Leakey REF. 1976. An Overview of the Hominidae from East Rudolf, Kenya. In: Coppens Y, and al. e, editors. Earliest Man and Environments in the Lake Rudolf Basin. Chicago: University of Chicago. p 476-483.

Lee SH. 2005. Brief communication: Is variation in the cranial capacity of the Dmanisi sample too high to be from a single species? American Journal of Physical Anthropology 127(3):263-266.
Lewis PO. 2001. A Likelihood Approach to Estimating Phylogeny from Discrete Morphological Character Data. Systematic Biology 50(6):913-925.
Lieberman DE, Wood BA, and Pilbeam DR. 1996. Homoplasy and early Homo: An analysis of the evolutionary relationships of H-habilis sensu stricto and H-rudolfensis. Journal of Human Evolution 30(2):97-120.
Lockwood CA. 1999. Sexual dimorphism in the face of Australopithecus africanus. American Journal of Physical Anthropology 108(1):97-127.
Maddison W, and Maddison D. 2007. Mesquite. www.mesquiteproject.org.
Mann AE. 1975. Paleodemographic Aspects of the South African Australopithecines. Philadelphia.
Mayr E. 1942. Systematics and the Origin of Speices. New York: Columbia University Press.
Mchenry HM. 1991. Femoral Lengths and Stature in Pliopleistocene Hominids. American Journal of Physical Anthropology 85(2):149-158.
Mckee JK. 1989. Australopithecine Anterior Pillars - Reassessment of the Functional-Morphology and Phylogenetic Relevance. American Journal of Physical Anthropology 80(1):1-9.
Miller JMA. 2000. Craniofacial variation Homo habilis: An analysis of the evidence for multiple species. American Journal of Physical Anthropology 112(1):103-128.
Olson TR. 1978. Hominid Phylogenetics and Existence of Homo in Member-I of Swartkrans Formation, South-Africa. Journal of Human Evolution 7(2):159-178.
Potts R, Behrensmeyer AK, Deino A, Ditchfield P, and Clark J. 2004. Small mid-Pleistocene hominin associated with east African Acheulean technology. Science 305(5680):75-78.
Prat S. 2002. Anatomical Study of the Skull of the Kenyan Specimen KNM-ER 1805: a Re-evaluation of its Taxonomic Allocation? Comptes Rendus de Palevol 1(27-33).
Prat S. 2005. Characterizing early *Homo*: cladistic, morphological and metrical analyses of the original Plio-Pleistocene specimens. In: Backwell L, and D'Errico F, editors. From tools to symbols, from hominids to modern humans. Johannesburg: Witwatersrand University Press. p 198-228.
Rightmire GP. 1998. Evidence from facial morphology for similarity of Asian and African representatives of Homo erectus. American Journal of Physical Anthropology 106(1):61-85.
Robinson JT. 1965. Homo Habilis and Australopithecines. Nature 205(4967):121-124.
Ronquist F, and Huelsenbeck JP. 2003. MrBayes 3: Bayesian phylogenetic inference under mixed models. Bioinformatics 19(12):1572-1574.
Rosas A. 2000. Ontogenetic Approach to Variation in Middle Pleistocene Hominids. Evidence from the Atapuerca-SH Mandibles. Human Evolution 15:83-98.
Schafer JL. 1997. Analysis of Incomplete Multivariate Data. London: Chapman & Hall.
Schafer JL. 1999. NORM: Multiple Imputation of Incomplete Multivariate Data Under a Normal Model, version 2. Software for Windows 95/98/NT, available from http://www.stat.psu.edu/~jls/misoftwa.html. Version 2.03.
Schafer JL, and Olsen MK. 1998. Multiple imputation for multivariate missing-data problems: A data analyst's perspective. Multivariate Behavioral Research 33(4):545-571.
Shennan S. 1997. Quantifying Archaeology. Iowa City: University of Iowa Press. 433 p.

Skinner MM, Gordon AD, and Collard NJ. 2006. Mandibular size and shape variation in the hominins at Dmanisi, Republic of Georgia. Journal of Human Evolution 51(1):36-49.
Smith HF, and Grine FE. 2008. Cladistic analysis of early Homo crania from Swartkrans and Sterkfontein, South Africa. Journal of Human Evolution 54(5):684-704.
Steudel K. 1980. New Estimates of Early Hominid Body Size. American Journal of Physical Anthropology 52(1):63-70.
Strait DS, and Grine FE. 2004. Inferring Hominoid and Early Hominid Phylogeny Using Craniodental Characters: the Role of Fossil Taxa. Journal of Human Evolution 47:399-452.
Strait DS, Grine FE, and Moniz MA. 1997. A reappraisal of early hominid phylogeny. Journal of Human Evolution 32(1):17-82.
Swofford DL. 2003. Paup*: Phylogenetic Analysis Using Parsimony (*and other methods). Sunderland, MA: Sinauer Associates.
Thompson JL. 1993. The Unusual Cranial Attributes of KNM-ER 1805 and Their Implication for Studies of Sexual Dimorphism in *Homo habilis*. Human Evolution 8:255-263.
Tinn O, and Oakley TH. 2008. Erratic rates of molecular evolution and incongruence of fossil and molecular divergence time estimates in Ostracoda (Crustacea). molecular Phylogenetics and Evolution.
Tobias PV. 1966. Distinctiveness of Homo Habilis. Nature 209(5027):953-957.
Tobias PV. 1973. New Developments in Hominid Paleontology in South and East-Africa. Annual Review of Anthropology 2:311-334.
Tobias PV. 1980. The Natural-History of the Helicoidal Occlusal Plane and Its Evolution in Early Homo. American Journal of Physical Anthropology 53(2):173-187.
Tobias PV. 1985. Single Characters and the Total Morphological Pattern Redefined: the Sorting Effected by a Selection of Morphological Features of the Early Hominids. Ancestors: the Hard Evidence: Alan R Liss. p 94-101.
White TD, Johanson DC, and Kimbel WH. 1981. Australopithecus-Africanus - Its Phyletic Position Reconsidered. South African Journal of Science 77(10):445-470.
Wolpoff MH. 1978. Some Aspects of Canine Size in Australopithecines. Journal of Human Evolution 7(2):115-126.
Wood B. 1992. Origin and Evolution of the Genus Homo. Nature 355(6363):783-790.
Wood BA. 1978. Classification and Phylogeny of East African Hominids. In: Chivers D, and Jowsey J, editors. Recent Advances in Primatology. New York: Academic Press. p 351-372.
Wood BA. 1991. Koobi Fora Research Project, volume 4: Hominid Cranial Remains. Oxford: Clarendon Press.
Wood BA, and Abbott SA. 1983. Analysis of the Dental Morphology of Plio-Pleistocene Hominids .1. Mandibular Molars - Crown Area Measurements and Morphological Traits. Journal of Anatomy 136(Jan):197-219.
Wood BA, Abbott SA, and Uytterschaut H. 1988. Analysis of the Dental Morphology of Plio-Pleistocene Hominids .4. Mandibular Post-Canine Root Morphology. Journal of Anatomy 156:107-139.
Wood BA, and Engleman CA. 1988. Analysis of the Dental Morphology of Plio-Pleistocene Hominids V. Maxillary Postcanine Tooth Morphology. Journal of Anatomy 161:1-35.
Wood BA, and Richmond BG. 2000. Human evolution: taxonomy and paleobiology. Journal of Anatomy 197:19-60.

TABLES

Table 1 . Taxonomic Allocation of Cranial and Mandibular Comparative Morphometric Sample

Cranial Specimens	***A priori* allocation**	**Mandibular Specimens**	***A. priori allocation***
AL 162-28	*A. afarensis*[1]	LH4	*A. afarensis*[1]
AL 333-45	*A. afarensis*[1]	AL 145-35	*A. afarensis*[12]
AL 444-2	*A. afarensis*[1]	AL 207-13	*A. afarensis*[12]
Sts 5	*A. africanus*[1]	AL 277-1	*A. afarensis*[12]
Sts 71	*A. africanus*[1]	AL 333W-1*	*A. afarensis*[12]
MLD 1	*A. africanus*[3]	AL 333W-60	*A. afarensis*[12]
MLD 37	*A. africanus*[3]	AL 400-1	*A. afarensis*[12]
Sts 1511	*A. africanus*[5]	Sts 52	*A. africanus*[1]
WT 17000	*P. boisei*[1]	MLD 2	*A. africanus*[15]
ER 13750	*P. boisei*[1]	MLD 40	*A. africanus*[3]
ER 406	*P. boisei*[1]	Sts 7	*A. africanus*[3]
ER 407	*P. boisei*[1]	Sts 36	*A. africanus*[3]
ER 732	*P. boisei*[1]	SK 61	*P. robustus*[14]
ER 23000	*P. boisei*[1]	SK 62	*P. robustus*[14]
OH 5	*P. boisei*[1]	SK 63	*P. robustus*[14]
Omo L338y-13	*P. boisei*[2]	SK 12	*P. robustus*[3]
SK 54	*P. robustus*[17]	SK 23	*P. robustus*[3]
SK 46	*P. robustus*[7]	OH 13	*H. habilis*[1]
SK 48	*P. robustus*[7]	OH 37	*H. habilis*[12]
SK 52	*P. robustus*[7]	ER 1482	*H. rudolfensis*[12]
SK 47	*P. robustus*[8]	ER 1483	*H. rudolfensis*[12]
ER 1813	*H. habilis*[1]	ER 1801	*H. rudolfensis*[12]
OH 16	*H. habilis*[1]	ER 819	*H. rudolfensis*[12]
OH 24	*H. habilis*[1]	BK 67	*H. erectus*[12]
OH 13	*H. habilis*[1]	Ternifine 1	*H. erectus*[12]
Stw 53	*H. habilis*[6]	Ternifine 2	*H. erectus*[12]
ER 1470	*H. rudolfensis*[1]	Ternifine 3	*H. erectus*[12]
ER3732	*H. rudolfensis*[1]	Dmanisi 2282	*H. erectus*[18]
OH 9	*H. erectus*[1]	ER 730	*H. ergaster*[1]
Sangiran 17	*H. erectus*[1]	ER 820	*H. ergaster*[1]
Dmanisi 2280	*H. erectus*[18]	ER 992	*H. ergaster*[1]
Dmanisi 2282	*H. erectus*[18]	OH 51	*H. ergaster*[12]
Dmanisi 2700	*H. erectus*[18]	ER 3734	*H. ergaster*[13]
Dmanisi 3444	*H. erectus*[18]	ER 1805	*Unknown*
OH 12	*H. erectus*[9]		
ER 3733	*H. ergaster*[1]		
ER 3883	*H. ergaster*[1]		
WT 15000	*H. ergaster*[1]		

ER 1805	*Unknown*

Table 1: [1](Wood and Richmond 2000); [2](Holloway 1981); [3](Kimbel et al. 1984); [4](Mchenry 1991); [5](Mckee 1989); [6](Lockwood 1999); [7](Steudel 1980); [8](de Ruiter et al. 2006); [9](Potts et al. 2004); [10](Huffman 2001); [11](Anton 2003); [12](Skinner et al. 2006); [13](Rosas 2000); [14](Dean 1985); [15](Tobias 1973); [16](Rightmire 1998); [17](Mann 1975); [18](Gabunia et al. 2000) ;presence of an asterisk (*) next to a specimen denotes that those measurements were taken from a cast; all others were taken from the originals.

Table 2. Taxonomic Allocation of Cladistic Sample

Cranial Specimens	***A. priori* Allocation**
AL 333-45	*A. afarensis*[1]
Stw505	*A. africanus*[1]
Sts 5	*A. africanus*[1]
Sts 71	*A. africanus*[1]
ER 406	*P. boisei*[1]
OH 5	*P. boisei*[1]
WT 17000	*P. boisei*[1]/*P. aethiopicus*[5]
SK 48	*P. robustus*[3]
SK 46	*P. robustus*[3]
ER 1813	*H. habilis*[1]
OH 24	*H. habilis*[1]
OH 13	*H. habilis*[1]
OH 16	*H. habilis*[1]
OH 62	*H. habilis*[1]
Stw 53	*H. habilis*[2]
ER 1470	*H. rudolfensis*[1]
ER 3732	*H. rudolfensis*[1]
OH 9	*H. erectus*[1]
ER 730	*H. ergaster*[1]
ER 3733	*H. ergaster*[1]
ER 3883	*H. ergaster*[1]
ER 1805	*Unknown*

Table 2: [1](Wood and Richmond 2000); [2](Lockwood 1999); [3](Steudel 1980); [4](Leakey et al. 2001); [5](Alemseged et al. 2002)

Table 3. Cladistic Characters and Coded State Decriptions from Prat (2005)

Trait	**Character States**
Cranium shape	(0) ovoid, (1) intermediate, (2) long
Cranial shape in norma occipitalis	(0) round, (1) trapezoidal, (2) lateral walls divergent on the upper part
Maximum cranial breadth	(0) mastoid, (1) parieto-temporal (2) parietal
Maximum biparietal breadth	(0) low, (1) medium, (2) high
Supraorbital torus	(0) absent, (1) present, continuous, (2) present, not continuous
Supraorbital torus prominence	(0) high, (1) medium, (2) weak
Supraorbitalis sulcus	(0) absent, (1) incomplete, (2) complete
Glabellar region in norma facialis	(0) straight, (1) rounded, (2) depression
Glabellar region in norma lateralis	(0) straight, (1) rounded, (2) depression
Prominence of the glabella	(0) not prominent , (1) medium, (2) prominent
Supraorbital depth	(0) shallow, (1) medium, (2) deep
Lateral postorbital depression	(0) absent, (1) present
Supratrigonal depression	(0) absent, (1) present
Fronto-temporale tubercle	(0) absent, (1) present
Frontal eminence	(0) absent, (1) present
Convexity of the frontal squama	(0) absent or weak, (1) strong
Metopic crest	(0) absent, (1) present
Postorbital constriction	(0) strong, (1) weak
Superior temporal lines on the supraorbital torus	(0) absent, (1) present
Parietal eminence	(0) absent, (1) present, medium position, (2) present, high position
Prelambdoid depression	(0) absent, (1) present
Torus angularis	(0) absent, (1) present
Sagittal crest on the anterior part of the line bregma-lambda	(0) present, (1) absent
Development of the sagittal crest	(0) weak, (1) medium, (2) strong
Maximal length of the parietal bone	(0) high, (1) low
Position of the temporal lines	(0) high, (1) medium, (2) low
Temporal lines or crests	(0) lines, (1) crests
Temporal lines position/parietal lines	(0) superior, (1) same level, (2) inferior
Shape of the temporal squama	(0) triangular and low, (1) rounded and high
Orientation of the anterior part of the temporal squama	(0) vertical, (1) anterior (2) posterior
Shape of the superior part of the temporal squama	(0) horizontal, (1) posterior
Lateral development of the supramastoid crest	(0) < 5 mm, (1)5 < d < 10 mm, (2) > 10 mm
Supramastoid development	(0) weak, (1) intermediate, (2) strong
Supramastoid development at porion	(0) absent, (1) present

Mastoid crest individualization	(0) absent, (1) weak, (2) strong
Supramastoid tubercle	(0) absent, (1) present
Junction between the mastoid and the supramastoid crests	(0) absent, (1) present
Slope of the zygomatic process of the temporal/ FH	(0) anterior, (1) parallel
Angle between the zygomatic process and the temporal process	(0) present, (1) absent
Shape of the posterior root of the zygomatic process	(0) elliptic, (1) flat, (2) circular
Position of the posterior root of the zygomatic process:	(0) postglenoid process, (1) between the postglenoid process and the anterior zygomatic tubercle, (2) porion
Inflection of mastoids beneath cranial base	(0) medial, (1) vertical, (2) lateral
Lateral projection of the mastoid with distinct sulcus	(0) absent, (1) present
Juxtamastoid eminence	(0) absent, (1) weak, (2) strong
Occipitomastoid suture/ juxtamastoid eminence	(0) middle, (1) lateral, (2) medial
Shape of the external meatus auditory	(0) rounded, (1) elliptic SA-IP, (2) elliptic AP, (3) elliptic SI, (4) elliptic AI-SP
Shape of the temporomandibular joint	(0) rectangular, (1) diamond-shaped
Development of the articular eminence	(0) ML=AP, (1)ML > AP, (2) ML >> AP, (3) ML < AP
Shape of the articular eminence	(0) straight, (1) 2 joint surfaces
Continuity between the posterior slope of the articular eminence and tympanic plate	(0) present, (1) absent
Entoglenoid process position	(0) entirely on the squamosal, (1) in part on the sphenoid
Fissure between the tympanic plate and the postglenoid process	(0) present, (1) absent
Position of the entoglenoid process apex and the corotid and ovale foramina axis	(0) lateral, (1) in the axis
Postglenoid process shape	(0) symmetrical, triangular, (1) asymmetrical laterally orientated, (2) rectangular
Position of the postglenoid process relative to the lateral part of the tympanic part of the temporal	(0) lateral, (1) same position, (2) medial
Position of the postglenoid apex relative to the middle of the articular eminence	(0) lateral, (1) middle
Existence of a preglenoid tubercle	(0) absent, (1) present, anterior part of the articular eminence, (2) present, forward the articular eminence
Mandibular fossa depth/ FH	(0) under, (1) same level, (2) above
Continuity of the mastoid fissure	(0) present, (1) absent
Mastoid process/ tympanic plate	(0) same surface, (1) fissure
Paramastoid process	(0) absent, (1) present
Petrous crest development	(0) absent, (1) present
Vaginal process	(0) absent, (1) present
Shape of the tympanic canal	(0) straight, (1) tubular, (2) crest

Eustachian process	(0) absent, (1) present
Shape of the foramen magnum	(0) oval, (1) heart-shaped
Position of the foramen magnum relative to the bitympanic line	(0) posterior, (1) same level, (2) anterior
Position of the basion relative to the PPG-PPG line	(0) same level, (1) posterior, close, (2) posterior, far
Inclination of nuchal plane	(0) near vertical, (1) near FH
Inclination of foramen magnum	(0) posterior, (1) anterior
Dimension nuchal plane/ occipital plane	(0) shorter, (1) longer
Inion / opisthocranion	(0) behind, (1) same level, (2) above
External occipital protuberance	(0) absent, (1) present
Occipital torus	(0) absent, (1) present, development in the medial part, (2) present, development in the medial and lateral parts
External occipital crest	(0) absent, (1) present, not continuous, (2) present, continuous
Linea suprema	(0) absent, (1) small lines, (2) developed
Compound temporal/ nuchal crest	(0) absent, (1) present
Asterionic notch	(0) absent, (1) present
Temporoparietal overlap of occipital at asterion	(0) absent, (1) present
Occipital bun	(0) absent, (1) present
Nasion approaches glabella	(0) yes, (1) no
Nasoalveolar clivus convexity	(0) concave, (1) straight, (2) convex
Maxillary trigon	(0) absent, (1) present
Maxillary groove	(0) absent, (1) present
Shape of the dental arch	(0) uspuloid, (1) parabolic
Canina fossa	(0) absent, (1) present
Infraorbital depression	(0) absent, (1) present
Alignment of canines and incisors	(0) yes, (1) only incisors, (2) no
Convexity of the alveolar part at the incisors level	(0) absent, (1) present
Anterior pillars	(0) absent, (1) present
Incisor region independent of pyriform aperture	(0) no, (1) yes
Facial prognathism	(0) weak, (1) strong
Position of the projection of the temporal process / pyriform aperture	(0) low, (1) middle, (2) high
Lateral zygomatic prominence	(0) absent, (1) present
Zygomaticomaxillary fossa	(0) absent, (1) present
Projection of the zygomatic bone	(0) anterior, (1) vertical, (2) posterior
Frontomaxillary position	(0) P4-M1, (1) M1-M2, (2) M2-M3
Orbital shape	(0) rectangular ML elongation, (1) rectangular SI elongation, (2) square
Superior orbital shape	(0) rectangular, (1) rounded, (2) ovoid
Orientation of the lateral margin of the orbits	(0) vertical, (1) medial
Orientation of the medial margin of the orbits	(0) vertical, (1) lateral

Position of the superior margin/ inferior margin of the orbit	(0) anterior, (1) same level, (2) posterior
Inferior orbital margin rounded laterally	(0) no, (1) yes
Multiple infraorbital foramen	(0) present, (1) absent
Anterior nasal spine	(0) absent, (1) present
Nasal eversion	(0) absent, (1) present
Shape of the lateral margin of the nasal aperture	(0) rounded, (1) sharped
Lateral expansion of the superior part of the nasal bones	(0) absent, (1) present
Location of the greatest width of the nasal bones	(0) inferior, (1) superior
Projection of the nasal bones relative to the frontomaxillary suture	(0) above, (1) same level, (2) under
Divided hypoglossal canal	(0) absent, (1) present
Paracondylar process	(0) absent, (1) present
Spine of the ligament of the dens of the axis	(0) absent, (1) present
Styloid process	(0) absent, (1) present
Pterygoid bridge	(0) absent, (1) present
1Endocranial processus of the jugular foramen	(0) absent, (1) present
Exocranial processus of the jugular foramen	(0) absent, (1) present
Spinosum and ovale foramina	(0) distinct, (1) not distinct
Infraorbital fissure	(0) absent, (1) present
Metopic suture	(0) absent, (1) present
Incisive suture closure (anterior part)	(0) present, (1) absent
Alveolar prognathism	(0) strong, (1) weak

Table 4. Linear Measurements of Cranium and Mandible

Cranial Measurement	**Mandibular Measurement**
cranial capacity (cubed root)	minimum symphyseal thickness
nasion – opisthocranion	corpus breadth at mental foramen (L)
nasion – bregma	corpus breadth at P3/P4 (L)
bregma – inion	corpus breadth at M1/M2 (L)
basion – lambda	body height at the symphysis
basion – inion	body height at M1/M2 (L)
bregma – lambda	mental foramen - alveolar margin (L)
lambda – inion	
lambda – opisthocranion	
auriculare – asterion	
bi-asterionic breadth	
nasal breadth (piriform aperture)	
maximum cranial breadth	
maximum frontal breadth	
minimum frontal breadth	
minimum orbital to alveolar height	
supraglabella – bregma arc	
bregma – lambda arc	
lambda – inion arc	
asterion – inion – asterion arc	

Table 5. Total Variance Explained by Principal Components for Raw Cranial Data

Component	Initial Eigenvalues			Extraction Sums of Squared Loadings		
	Total	% of Variance	Cumulative %	Total	% of Variance	Cumulative %
1	10.163	50.817	50.817	10.163	50.817	50.817
2	3.370	16.849	67.667	3.370	16.849	67.667
3	1.669	8.343	76.010	1.669	8.343	76.010
4	1.093	5.466	81.476	1.093	5.466	81.476
5	.862	4.311	85.787	.862	4.311	85.787
6	.717	3.587	89.374	.717	3.587	89.374
7	.505	2.523	91.896	.505	2.523	91.896
8	.385	1.923	93.819	.385	1.923	93.819
9	.282	1.412	95.231	.282	1.412	95.231
10	.202	1.010	96.241	.202	1.010	96.241
11	.186	.931	97.173	.186	.931	97.173
12	.136	.682	97.855	.136	.682	97.855
13	.112	.558	98.413	.112	.558	98.413
14	.085	.427	98.840	.085	.427	98.840
15	.065	.326	99.166	.065	.326	99.166
16	.054	.268	99.434	.054	.268	99.434
17	.047	.233	99.667	.047	.233	99.667
18	.029	.146	99.814	.029	.146	99.814
19	.022	.111	99.925	.022	.111	99.925
20	.015	.075	100.000			

Table 6. Total Variance Explained by Principal Components for Raw Mandibular Data

Component	Initial Eigenvalues			Extraction Sums of Squared Loadings		
	Total	% of Variance	Cumulative %	Total	% of Variance	Cumulative %
1	4.883	69.752	69.752	4.883	69.752	69.752
2	1.126	16.082	85.833	1.126	16.082	85.833
3	.432	6.173	92.006	.432	6.173	92.006
4	.325	4.644	96.650	.325	4.644	96.650
5	.148	2.107	98.757	.148	2.107	98.757
6	.064	.920	99.677	.064	.920	99.677
7	.023	.323	100.000			

Table 7. Total Variance Explained by Principal Components for Transformed Cranial Data

Component	Initial Eigenvalues			Extraction Sums of Squared Loadings		
	Total	% of Variance	Cumulative %	Total	% of Variance	Cumulative %
1	6.289	31.447	31.447	6.289	31.447	31.447
2	3.504	17.522	48.969	3.504	17.522	48.969
3	2.172	10.860	59.829	2.172	10.860	59.829
4	1.534	7.671	67.500	1.534	7.671	67.500
5	1.253	6.267	73.767	1.253	6.267	73.767
6	1.102	5.508	79.276	1.102	5.508	79.276
7	.990	4.948	84.223	.990	4.948	84.223
8	.754	3.769	87.993	.754	3.769	87.993
9	.513	2.564	90.557	.513	2.564	90.557
10	.474	2.368	92.925	.474	2.368	92.925
11	.378	1.889	94.814	.378	1.889	94.814
12	.275	1.377	96.191	.275	1.377	96.191
13	.199	.997	97.188	.199	.997	97.188
14	.179	.896	98.085	.179	.896	98.085
15	.129	.645	98.730	.129	.645	98.730
16	.110	.551	99.280	.110	.551	99.280
17	.068	.340	99.620	.068	.340	99.620
18	.042	.208	99.828	.042	.208	99.828
19	.034	.172	100.000	.034	.172	100.000
20	-7.32E-017	-3.66E-016	100.000			

Table 8. Total Variance Explained by Principal Components for Transformed Mandibular Data

Component	Initial Eigenvalues			Extraction Sums of Squared Loadings		
	Total	% of Variance	Cumulative %	Total	% of Variance	Cumulative %
1	3.780	54.003	54.003	3.780	54.003	54.003
2	1.259	17.992	71.995	1.259	17.992	71.995
3	1.057	15.094	87.089	1.057	15.094	87.089
4	.545	7.784	94.873	.545	7.784	94.873
5	.254	3.622	98.495	.254	3.622	98.495
6	.105	1.505	100.000	.105	1.505	100.000
7	6.18E-017	8.83E-016	100.000			

Table 9. Predicted Group Membership for KNM-ER 1805 with Posterior and Typicality Probabilities

Data	**Group Allocation**	**Posterior Probability**	**Typicality Probability**
Raw Cranial	*A. africanus*	0.585	0.026
Transformed Cranial	*H. ergaster*	0.882	0.116
Raw Mandibular	*H. habilis*	0.996	0.000
Transformed Mandibular	*H. habilis*	0.996	0.000

FIGURE CAPTIONS

Figure 1. a) scatterplot of discriminant functions one and two for untransformed cranial measures; b) scatterplot of functions one and two with narrower scale to focus on groupings within fossil hominins.

Figure 2. a) scatterplot of discriminant functions one and two for untransformed mandibular measures; b) scatterplot of functions one and two with narrower scale to focus on groupings within fossil hominins.

Figure 3. a) scatterplot of discriminant functions one and two for transformed cranial measures; b) scatterplot of functions one and two with narrower scale to focus on groupings within fossil hominins.

Figure 4. a) scatterplot of discriminant functions one and two for transformed mandibular measures; b) scatterplot of functions one and two with narrower scale to focus on groupings within fossil hominins.

Figure 5. Maximum likelihood tree produced in CONTML from first ten principal components of untransformed cranial data.

Figure 6. Maximum likelihood tree produced in CONTML from first 12 principal components of transformed cranial data.

Figure 7. Maximum likelihood tree produced in CONTML from first five principal components of untransformed mandibular data.

Figure 8. Maximum likelihood tree produced in CONTML from first six principal components of transformed mandibular data.

Figure 9. Majority consensus tree produced from three most parsimonious trees recovered from maximum parsimony analysis using Paup 3.1, published in Prat (2002, 2005).

Figure 10. Single most parsimonious tree produced from maximum parsimony analysis using Paup* (4.10b) with Bremer decay index calculated for each of the nodes.

Figure 11. Consensus tree based upon Bayesian inferences methods with clade credibility values produced using MrBayes 3.1.2 program

FIGURES

Figure 1. Scatterplot of Discriminant Functions for Untransformed Cranial Measures

a.

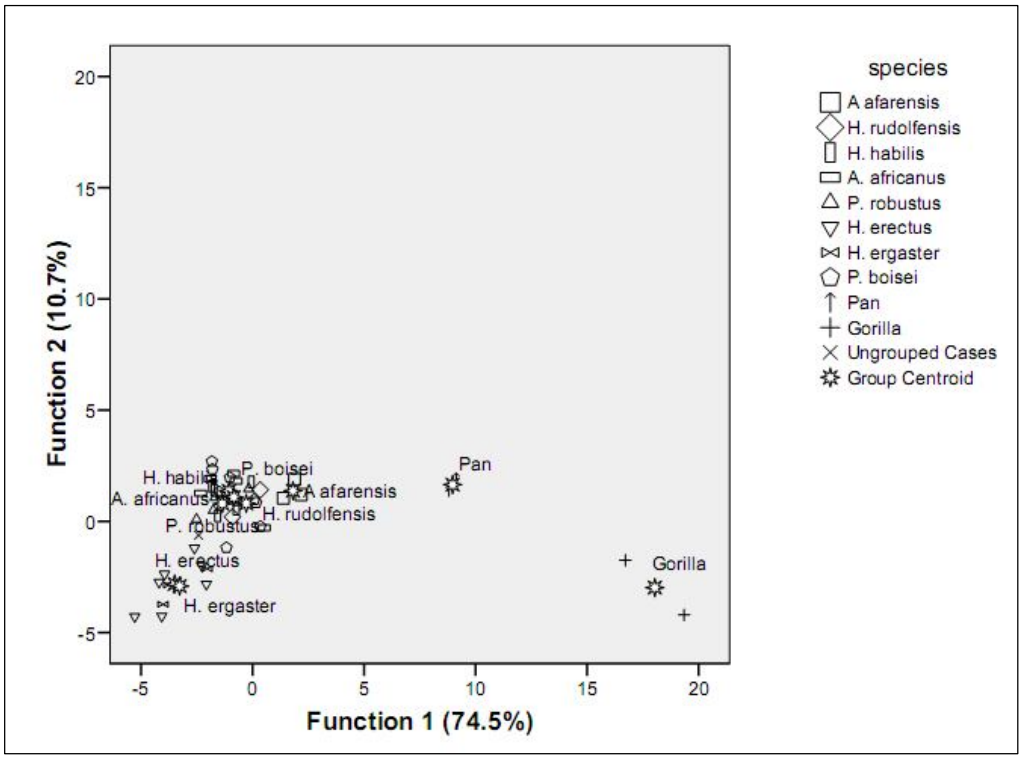

b.

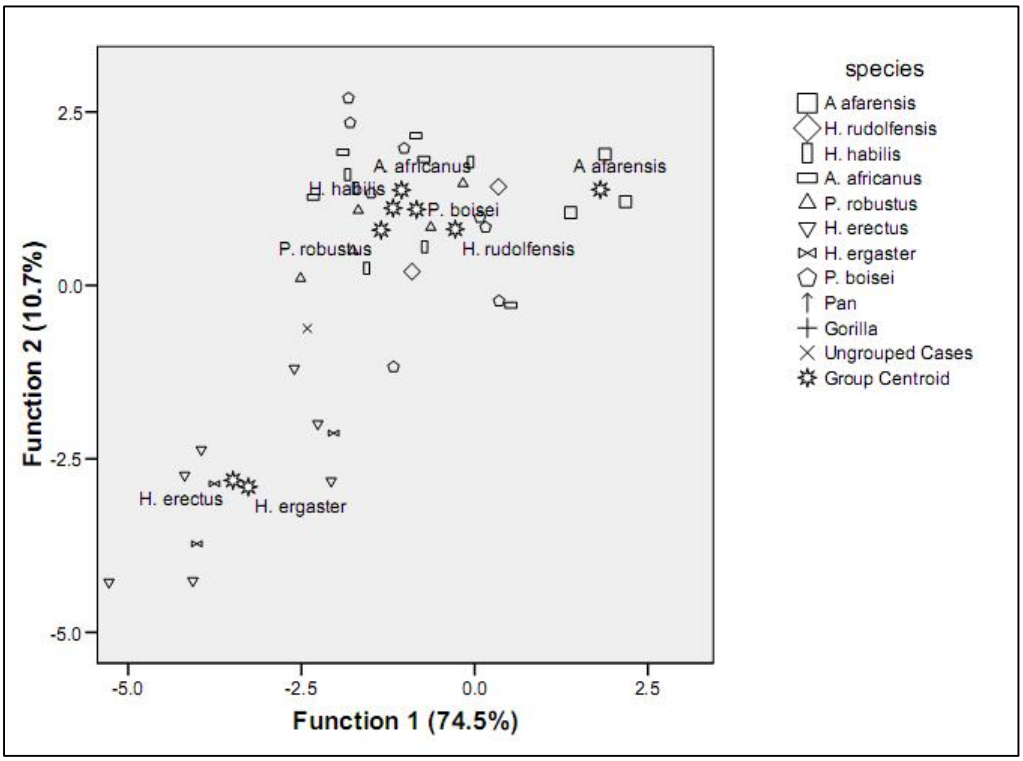

Figure 2. Scatterplot of Discriminant Functions for Untransformed Mandibular Measures

a.

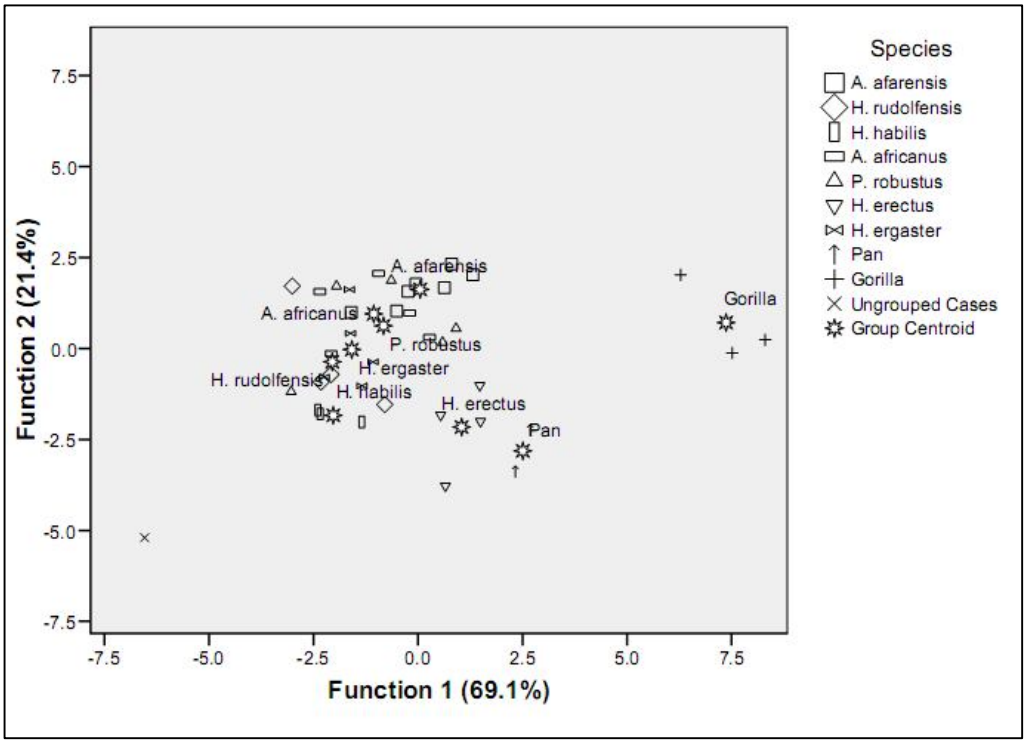

b.

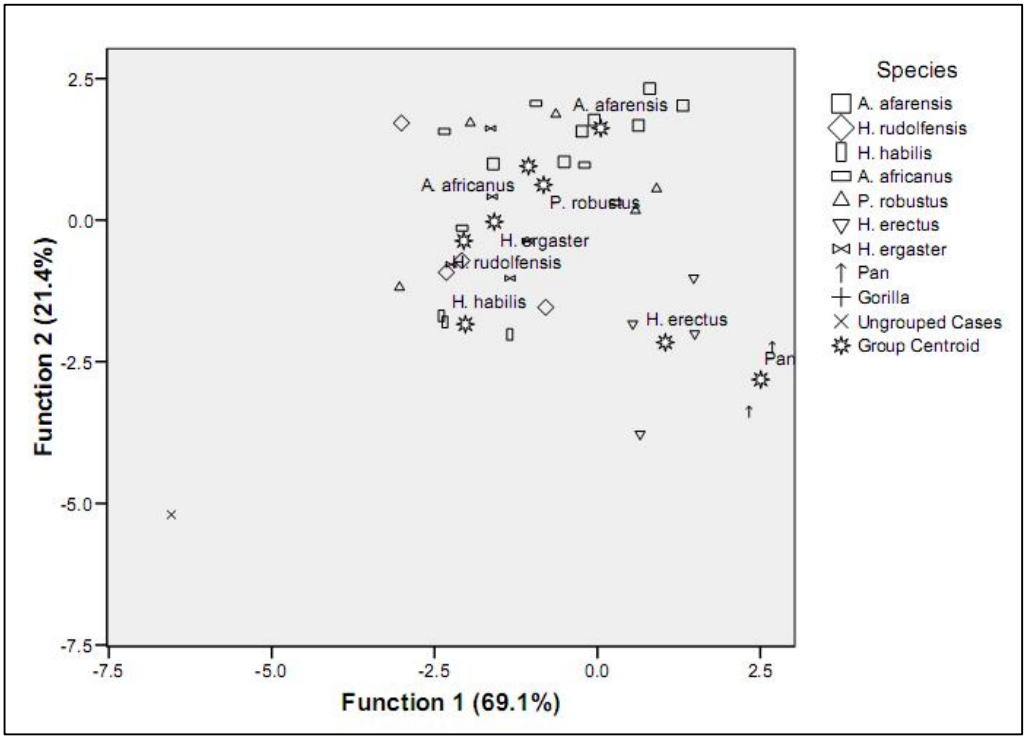

Figure 3. Scatterplot of Discriminant Functions for Transformed Cranial Measures

a.

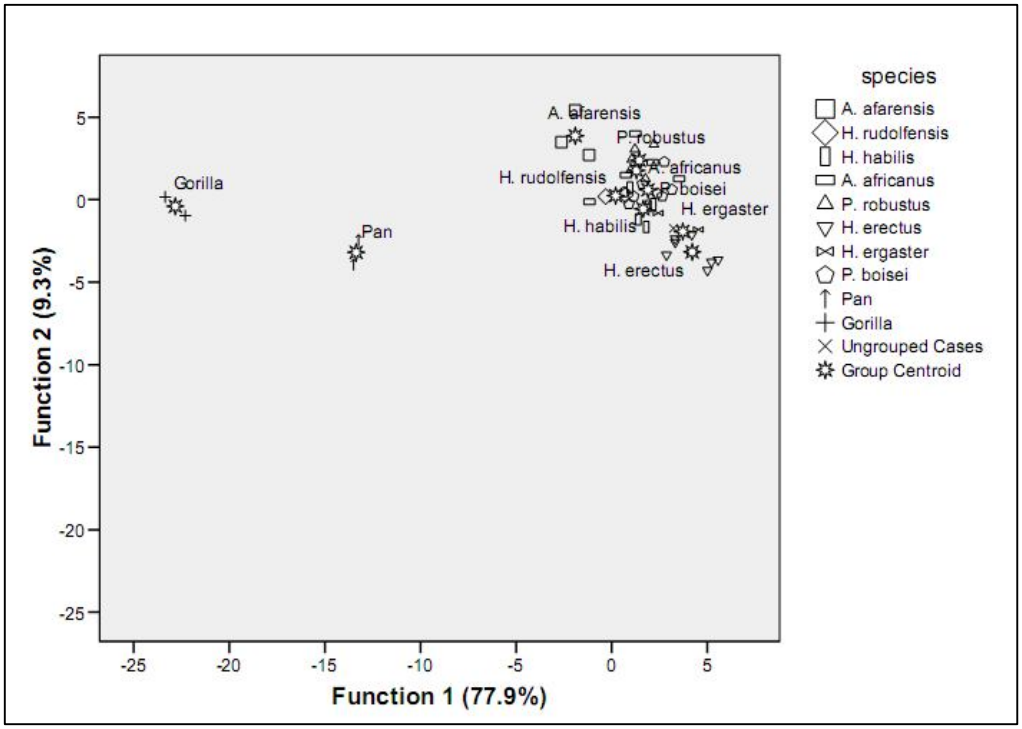

b.

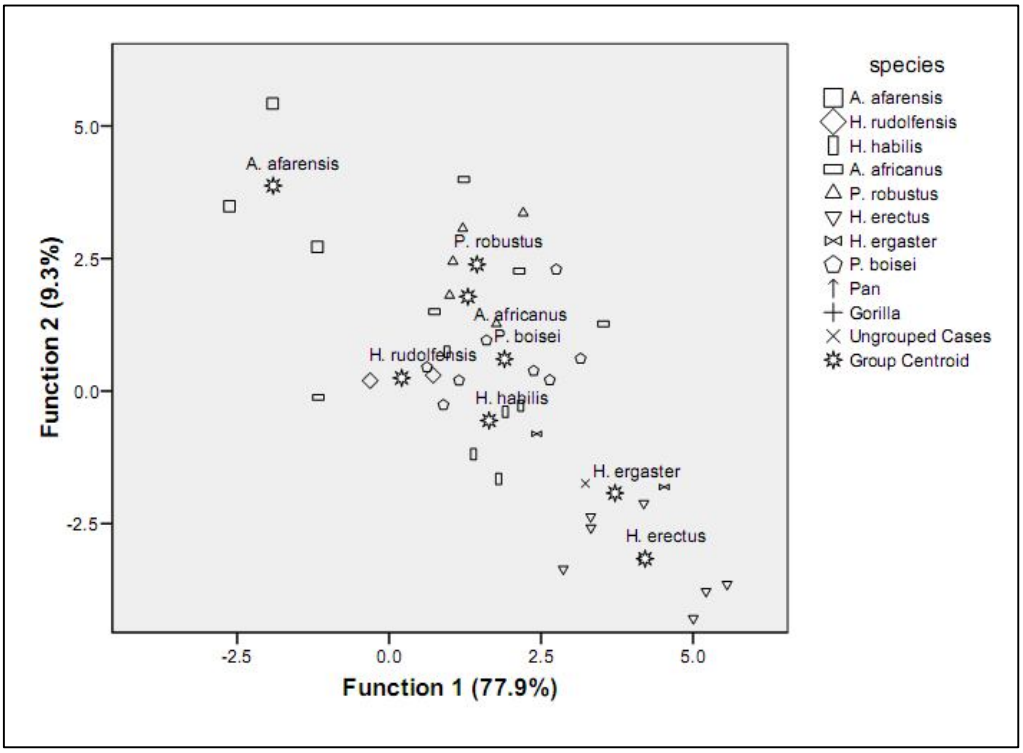

Figure 4. Scatterplot of Discriminant Functions for Transformed Mandibular Measures

a.

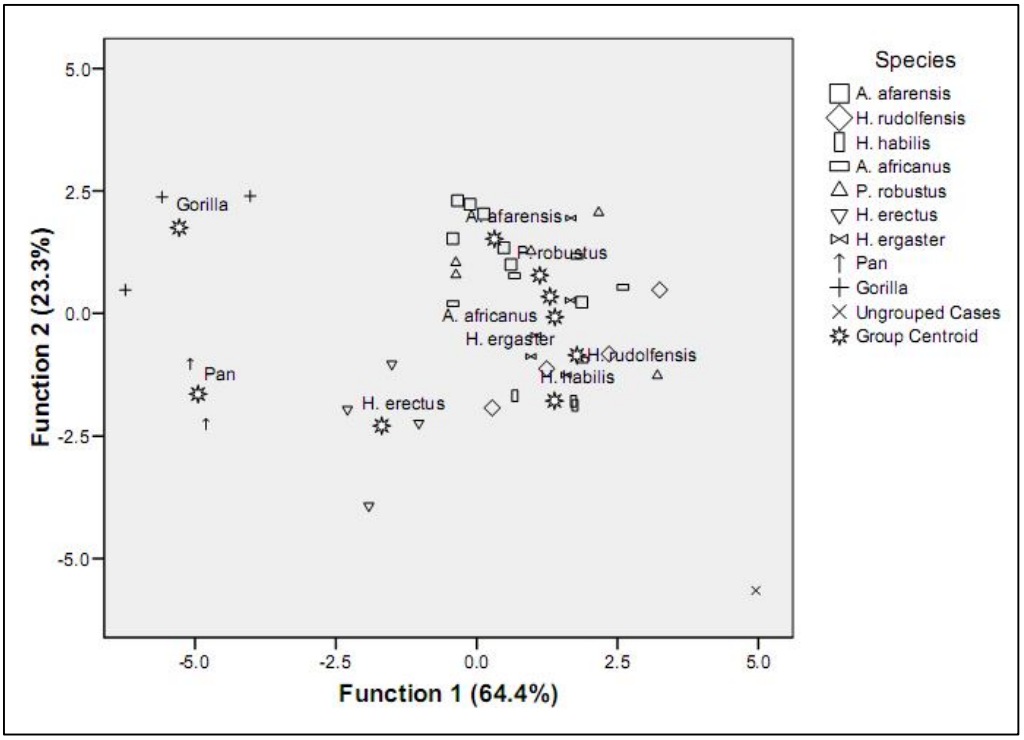

b.

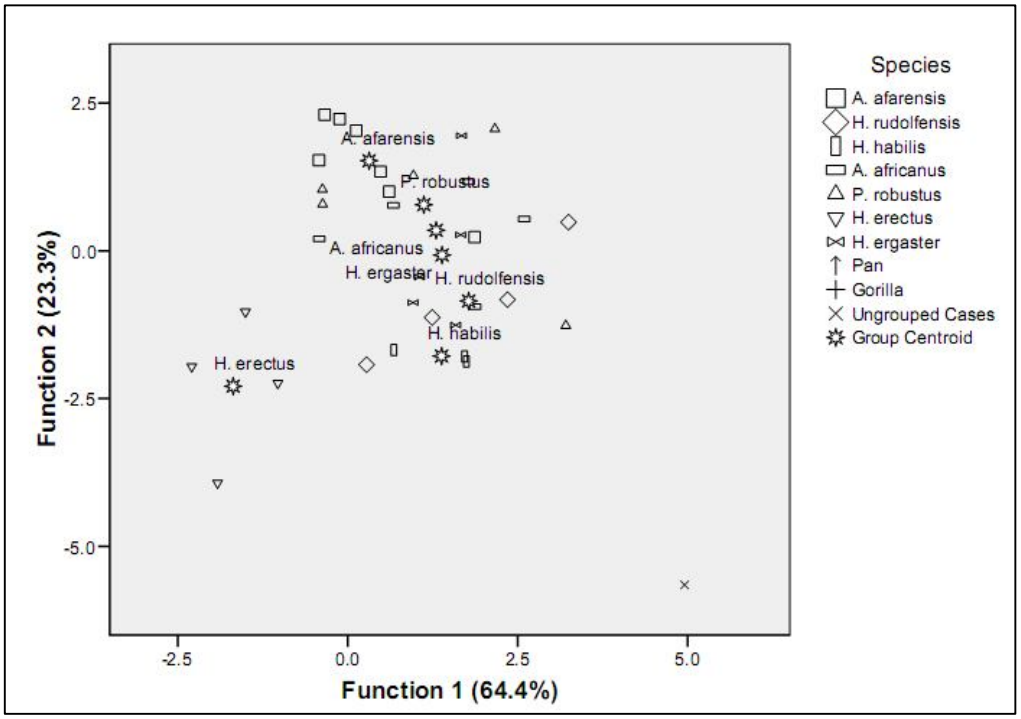

Figure 5. CONTML Tree from PC scores of Untransformed Cranial Data

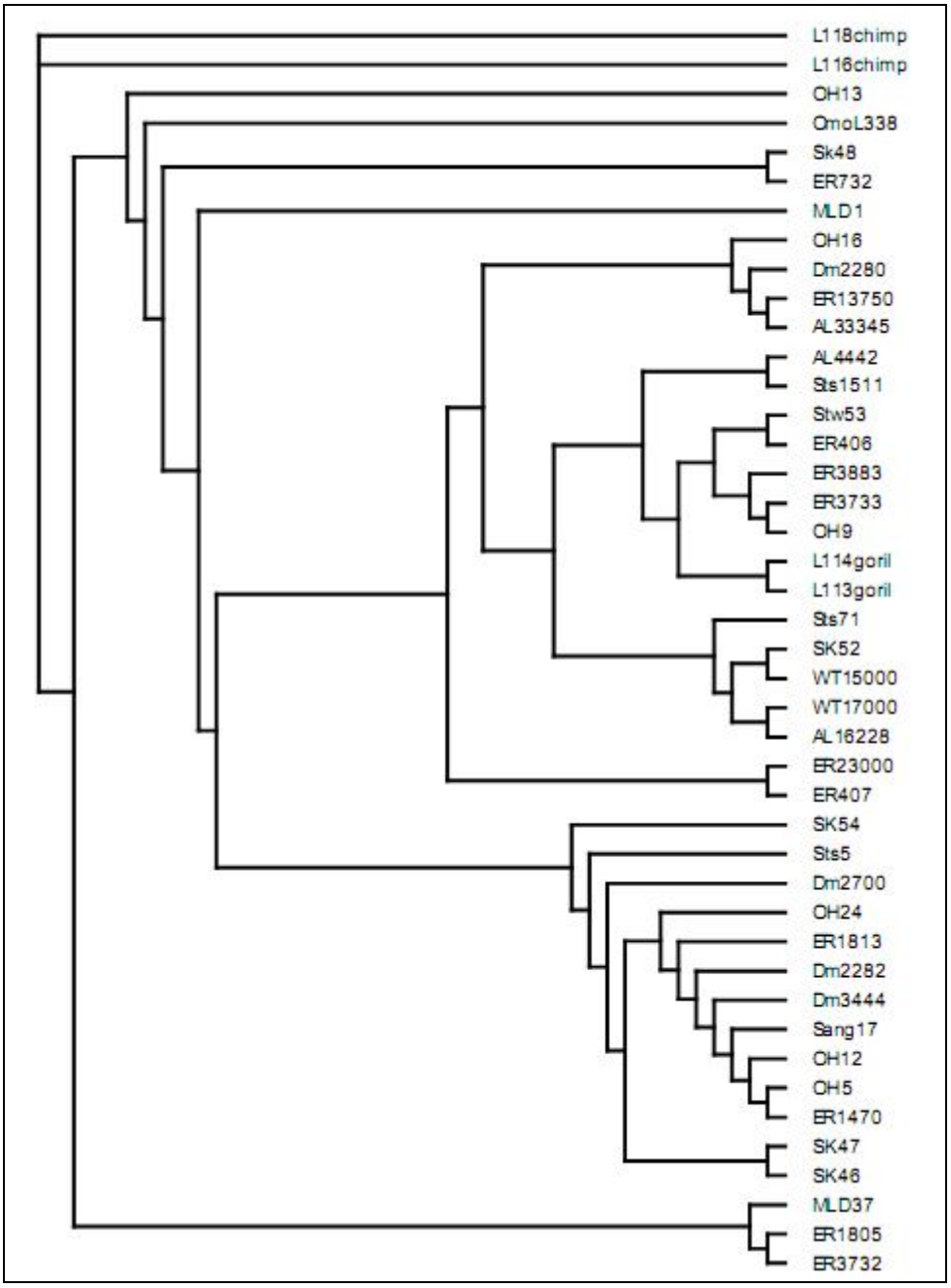

Figure 6. CONTML Tree from PC scores of Transformed Cranial Data

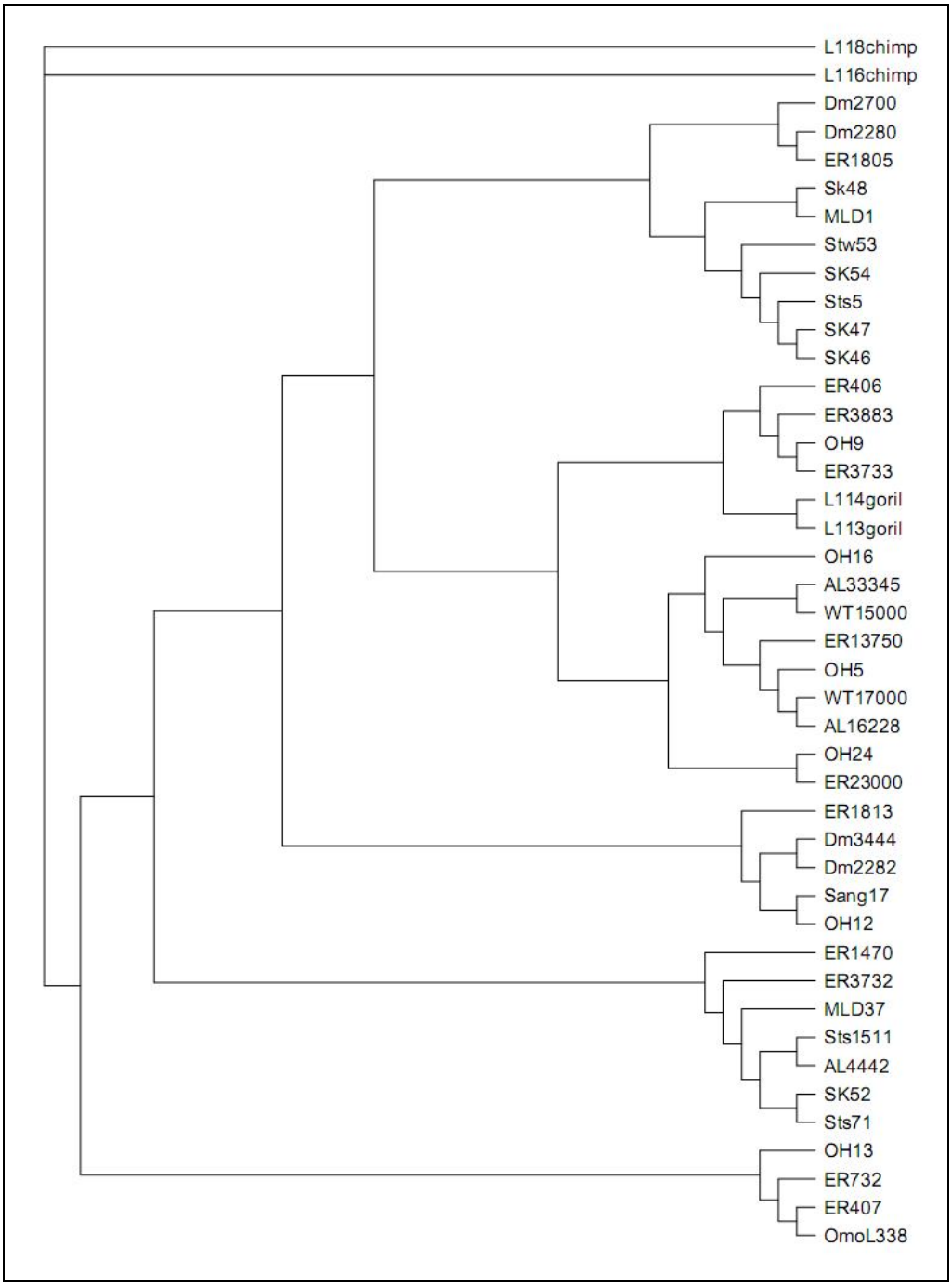

Figure 7. CONTML Tree from PC scores of Untransformed Mandibular Data

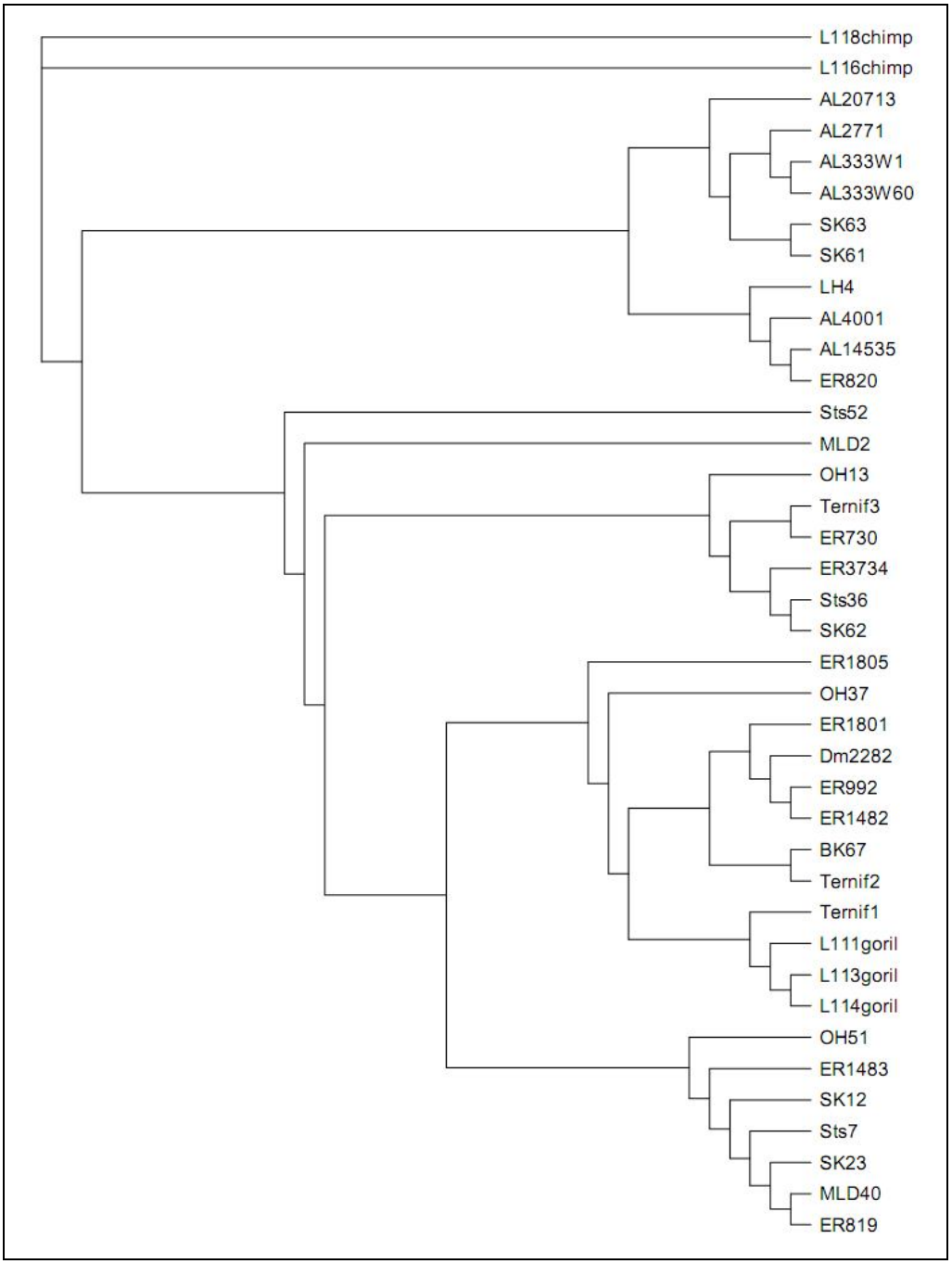

Figure 8. CONTML Tree from PC scores of Transformed Mandibular Data

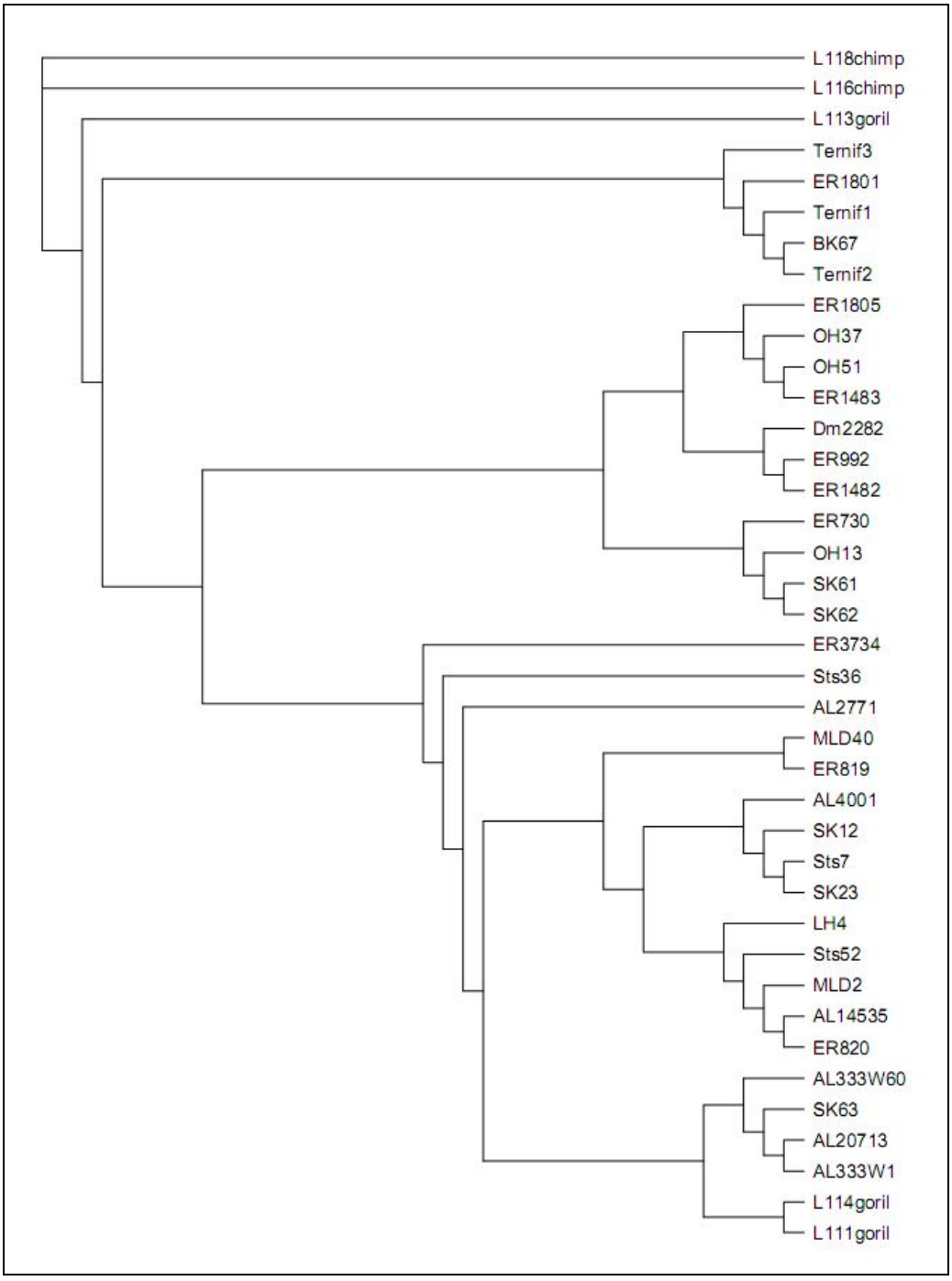

Figure 9. Consensus Tree of Three Most Parsimonious Trees from Prat (2002, 2005)

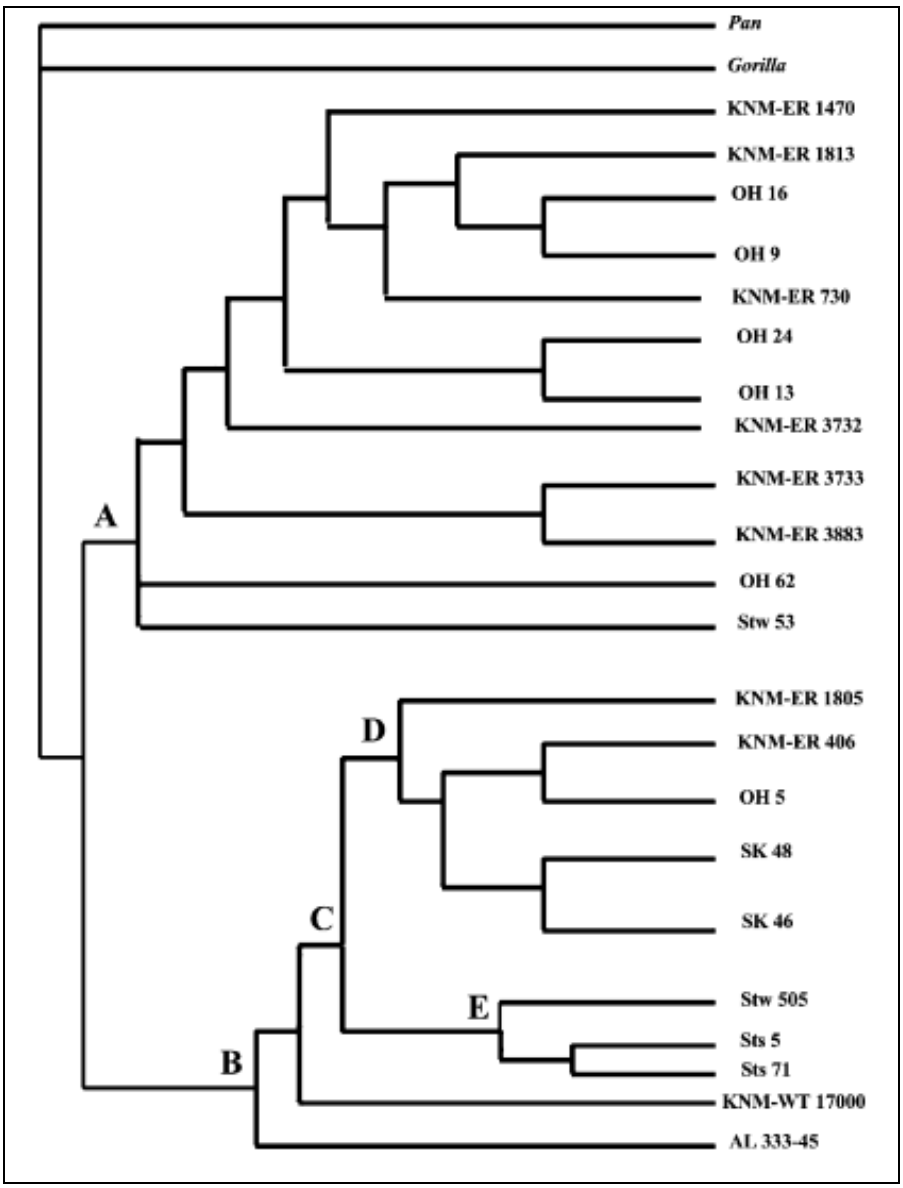

Length = 431 steps
CI = 0.452

Figure 10. Single Most Parsimonious Tree with Bremer Support at Nodes

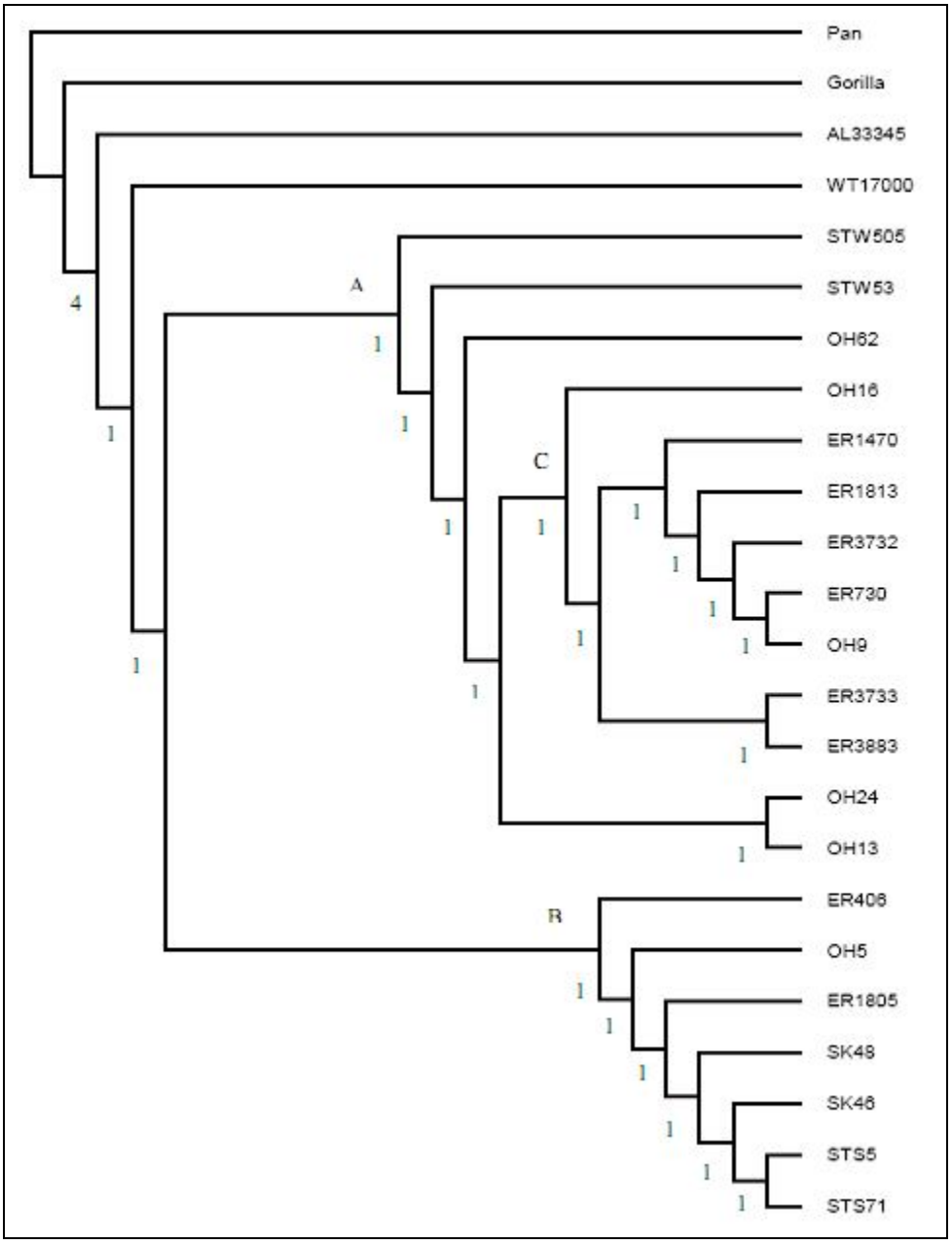

Length = 429 steps
CI = 0.452

Figure 11. MrBayes Consensus Tree with Clade Credibility Values